

**Design and Synthesis of Novel Functionalized Sensors
for the Biological Imaging of Zinc(II) and Nitric Oxide**

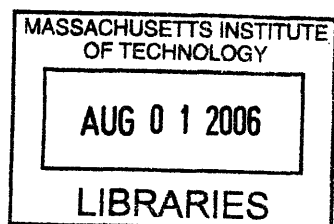
by

Annie C. Won

SUBMITTED TO THE DEPARTMENT OF CHEMISTRY
AT THE
MASSACHUSETTS INSTITUTE OF TECHNOLOGY

April 2005

June 2005



© Massachusetts Institute of Technology, 2005
All rights reserved

Signature of Author: _____

Department of Chemistry
April 29, 2005

Certified By : _____

Stephen J. Lippard
Arthur Amos Noyes Professor of Chemistry & Dept. Head
Thesis Supervisor

Approved by : _____

Rick L. Danheiser
Arthur C. Cope Professor & Assoc. Head of Chemistry

**Design and Synthesis of Novel Functionalized Sensors
for the Biological Imaging of Zinc(II) and Nitric Oxide**

by

Annie C. Won

Submitted to the Department of Chemistry on April 29, 2005

Abstract

CHAPTER 1: Fluorescent Sensors for the Biological sensing of Zinc(II)

A variety of fluorescent techniques have been developed for the *in vivo* sensing of Zn^{2+} . This chapter presents a brief overview of techniques used to image chelatable zinc(II) in neuronal cells. Ratiometric sensors have been developed for more precise zinc sensing. These sensors exhibit differentiable changes in fluorescence in the presence and absence of zinc.

CHAPTER 2. An Esterase-Activated System for the Ratiometric Sensing of Biological Zinc

A ratiometric two-fluorophore sensing system has been developed by coupling Zinpyr-1, a zinc-sensitive fluorophore, to the zinc-insensitive coumarin-343. The two fluorophores are bound by an ester linkage, which allows cell permeability; cytoplasmic esterases hydrolyze the sensor into its parent fluorophores.

CHAPTER 3: Syntheses of Zinpyr Derivatives for Localized Applications in Zn^{2+} Sensing

This chapter describes the preparation of reactive Zinpyr-1 derivatives for the direct functionalization of biological targets. A Zinpyr alkyne has been synthesized as a click chemistry substrate to couple to azides, and a Zinpyr succinimidyl ester has been developed to couple to amines. Applications of these derivatives include directly coupling the derivatives to glutamate receptor antagonists and small peptides for more localized sensing applications.

CHAPTER 4: Conjugated Polymer-Based Sensors for the Biological Imaging of NO

A variety of monomers featuring hydrophilic constituents have been synthesized for use in polymer synthesis via Pd-catalyzed cross-coupling reactions. CP-transition metal complexes have been made, using a variety of CPs including poly(p-phenylene vinylenes) (PPVs) and poly(p-phenylene ethynyls) (PPEs). Metal binding functionalities have been incorporated into the conjugate polymer main chains. The optical properties of the CPs have been examined, as well as the interactions of these CP-metal complexes with NO.

Acknowledgements

*"Sorrow happens, hardship happens, the hell with it,
who never knew the price of happiness,
will not be happy."
(Yevgeny Yevtushenko)*

I must admit, my happiest and most productive time at MIT has been applied to undergraduate research at the Lippard Lab, and for this opportunity, I thank Prof. Stephen J. Lippard. My first couple semesters of research in the neurochemistry subgroup ultimately motivated me to leave my (former) major (brain and cognitive sciences), and to gather the courage to pursue organic chemistry under the guidance of a renegade organic chemist, under the auspices of one of the best bioinorganic laboratories in the country.

I would like to thank past and present members of Team Neurochem for their encouragement and support; Liz Nolan, for helping to read my first UROP proposal; Erik Dill for late-night company; Mi Hee Lim and Viviana Izzo for their cheerful Korean/Italian insanity; Matt Clark, for his drunken antics during my first UROP group meeting; Chris Chang, for his undying bitterness and humor; Ben Davis and Scott Hilderbrand, for allowing me to capture photographs of them at Gay Head, followed by subsequent distribution; Jyoti Tibrewala and others for their presence as fellow UROPs and friends; Andy Tennyson, to whom I still owe a Hot Asian girl; Todd ("Thorrop") Harrop; Chris ("Notorious CRG") Goldsmith –

I would like to thank my first mentor, Carolyn ("Lynne") Woodroffe, for the opportunity to begin work with a synthesis project that taught me the chemistry of failure and the challenges of moving through revisions – from paper acceptance, to proofs, to publication. Many thanks go to Rhettinold C. (aka "Rhett") Smith for putting up with me; Rhett has been an Outstanding mentor with an incredible (and dangerous) combination of self-effacing humor, intelligence, experience, dedication, and martial arts skills –

I would like to thank the entire Lippard lab for allowing me to feed them cookies. I would like to thank my friends (MIT and otherwise) for reluctantly allowing me to think that there is never too much lab work – that there is never enough to do, and for that, I am grateful. I would like to thank those who believe that I can do chemistry, and who supported me on the journey towards graduate school, which I will be attending in the coming fall –

Lastly, I would like to thank my boyfriend, Doug Kavendek, for his undying chivalry and crazy long-distance commitment and the notion that I can be stolen away from Boston on various weekends – for introducing Team Neurochem Movie Night to our group, and for his experience in tying knots and excellent photography—of stuffed animals, and all such things.

And to everyone else, who should know who they are –
Or who knew enough to have helped me this far.

Table of Contents

Abstract.....	2
Acknowledgements.....	3
Table of Contents.....	4
Chapter 1: Fluorescent Sensors for the Biological sensing of Zinc(II)	5
Chapter 2: An Esterase-Activated System for the Ratiometric Sensing of Biological Zinc.....	15
Chapter 3: Syntheses of Zinpyr Derivatives for Localized Applications in Zn ²⁺ Sensing	29
Chapter 4: Conjugated Polymer-Based Sensors for the Biological Imaging of NO.....	41
Biographical Note.....	62
Curriculum Vitae.....	63

CHAPTER 1: Fluorescent Sensors for Biological Zinc(II) Sensing

CHAPTER 1: Fluorescent Sensors for Biological Zinc(II) Sensing

Zn^{2+} is one of the most important first row transition metals in biology. It is highly regulated under normal physiological conditions.¹ Prolonged deficiencies may result in problems such as impaired physical growth and severe immune defects.² Intracellular Zn^{2+} is found tightly bound to metalloproteins, or present as cytosolic free zinc at the subfemtomolar level.^{3,4} Unexpectedly high levels of zinc are present in the synaptic vesicles of the mossy fiber region of the hippocampus.⁵ Presynaptic Zn^{2+} has been implicated in the exacerbation of excitotoxic neuron injury and acceleration of plaque formation in Alzheimer's disease.⁶

Due to the spectroscopically silent nature of zinc, it is difficult to study. Zn^{2+} has no unpaired electrons for EPR or d-d transitions for optical studies.⁷ The zinc nucleus has poor NMR sensitivity, and radioactive methods cannot be used, due to low turnover rates of zinc in the brain. Autometallographic and fluorescence techniques have been developed to image free or loosely bound Zn^{2+} . The use of fluorescent biosensors provides several advantages over autometallography, in that unlike the latter process, fluorescent sensors do not involve irreversible processes or relatively harsh conditions.⁸

The following criteria have been defined for the development of fluorescent zinc sensors.⁷ The sensors must be stable, highly fluorescent, and selective for zinc in the presence of other biological cations (ex. Na^+ , K^+ , Ca^{2+} , and Mg^{2+}). When standard one-photon excitation is used, the excitation wavelengths of the sensors should exceed 340 nm to avoid UV wavelengths

¹ Vallee, B. L.; Falchuk, K. H. *Physiol. Rev.* **1993**, *73*, 79-118

² Hambridge, M. *J. Nutr.* **2000**, *130*, 1344S-1349S

³ Kambe, T.; Yamaguchi-Iwai, Y.; Sasaki, R.; Nagao, M. *Cell. Mol. Life Sci.* **2004**, *61*, 49-68

⁴ Outten, C. E.; O'Halloran, T. V. *Science* **2001**, *292*, 2488-2492

⁵ McLardy, T. *Acta Neurochir* **1970**, *23*, 119-124

⁶ Frederickson, C. J.; Bush, A. I. *BioMetals* **2001**, *14*, 353-266

⁷ Kimura, E.; Koike, T. *Chem. Soc. Rev.* **1998**, *27*(3), 179-184

⁸ Danscher, G.; Juhl, S.; Stoltenberg, M.; Krunderup, B.; Schroder, H. D.; Andreasen, A. *J. Histochem. Cytochem.* **1997**, *45*, 1503-1510

of light, and the dissociation constants of these probes should be near the median concentration of the desired analyte.

A landmark discovery in biological zinc sensing was the development of TSQ (Figure 1).⁹ It is a quinoline-based fluorescent sensor that can stain frozen and fixed tissues; however, it cannot be used with live cells. To become cell-permeable, molecules are often esterified. Cell-permeable TSQ-analogs such as Zinquin (Figure 1)¹⁰ have been among the first to use this strategy; Zinquin incorporates an ethyl ester moiety for cellular uptake, and consequent intracellular retention of the hydrolyzed species. This intensity-based probe has been successfully used in imaging live cells; however, its excitation wavelength lies in the ultraviolet range, which can potentially harm the cells. Studies of the coordination chemistry of Zinquin¹¹ have found that the sensor forms non-stoichiometric complexes with Zn^{2+} , making the quantitation of zinc difficult.

Following the independent syntheses of Zinpyr-1 and Zinpyr-2 in 1999,¹² our laboratory has significantly developed the Zinpyr (ZP) family of sensors (Figure 5). The Zinpyrs are PET-based (Figure 4) zinc sensors with two dipicolylamine (DPA) binding sites. Zinpyr compounds are excited at visible wavelengths of light and have a high (sub-nanomolar) affinity for Zn^{2+} . The first binding event causes the fluorescence of the compound to increase. The probes have relatively high background fluorescence, possibly due to the high pK_a values (8.4 and 9.4) (**3a**

⁹ Frederickson, C. J.; Kasarskis, E. J.; Ringo, D.; Frederickson, R. E. *J. Neurosci. Methods* **1987**, *20*, 91-103

¹⁰ Zalewski, P. D.; Millard, S. H.; Forbes, I. J.; Kapaniris, O.; Slavotinek, A.; Betts, W. H.; Ward, A. D.; Lincoln, S. F.; Mahadevan, I. *J. Histochem. Cytochem.* **1994**, *42*, 877-884.

¹¹ Fahrni, C. J.; O'Halloran, T. V. *J. Am. Chem. Soc.* **1999**, *121*, 11448-11458.

¹² Walkup, E.; Burdette, S.; Lippard, S.; Tsien, R. *J. Am. Chem. Soc.* **2000**, *122*, 5644-5645

and **3b**) of their benzylic amines. Cell-permeable and cell-impermeable versions of these sensors are readily available.¹³

Several strategies have been employed in the recent development of zinc sensors. A carbonic anhydrase-based sensor has been synthesized which binds Zn^{2+} with picomolar affinity (Figure 2).¹⁴ Ratiometric sensors have also been of interest; these sensors have easily differentiable fluorescent signals in the presence and absence of analyte. Fahrni and coworkers have reported ratiometric benzimidazole-based probes (Figure 3) which undergo a fast excited-state intramolecular proton transfer (ESIPT) (Figure 4) to their tautomers with high quantum yields (0.5).¹⁵ This sensing system suffers several drawbacks, in that it is only ratiometric in alcoholic environments, and cannot be used under physiological conditions.

In efforts to expand the capability of our sensors, Zinpyr-1-based ratiometric probes have been recently studied by our group for more precise measurements of intracellular zinc concentration. These probes incorporate zinc-sensitive and zinc-insensitive fluorophores that are coupled through ester linkages. Derivatives of Zinpyr-1 have also been sought for more localized sensing applications, such as zinc flux at receptor sites and specific intracellular regions. Recently developed methods such as click chemistry¹⁶ have been investigated in coupling the Zinpyr to small molecules with localization capability, such the RGD peptide. Activated, isolable intermediates of Zinpyr-1 have also been investigated and found to be effective when coupled to amines—particularly NMDA antagonists. Coupled Zinpyr-antagonist products may be used to monitor zinc flux at receptor sites, for more specific elucidation of the concentrations and

¹³ Chang, C. J.; Nolan, E. M.; Jaworski, J.; Okamoto K.; Hayashi, Y.; Sheng, M.; Lippard, S. J. *Inorg. Chem.* **2004**, *43*, 6774-9.

¹⁴ Fierke, C. A.; Thompson, R. B. *BioMetals* **2001**, *14*, 205-222.

¹⁵ Henary, M. M.; Fahrni, C. J. *J. Phys. Chem. A* **2002**, *106*, 5210-5220.

¹⁶ Hartmuth C. Kolb, Dr., Finn, M. G., Sharpless, K. *Barry. Angewandte Chemie International Edition* **2000**, *40*(11), 2004-2021

pathways of zinc in synaptic regions. The employment of these strategies will be discussed in further detail in the following chapters.

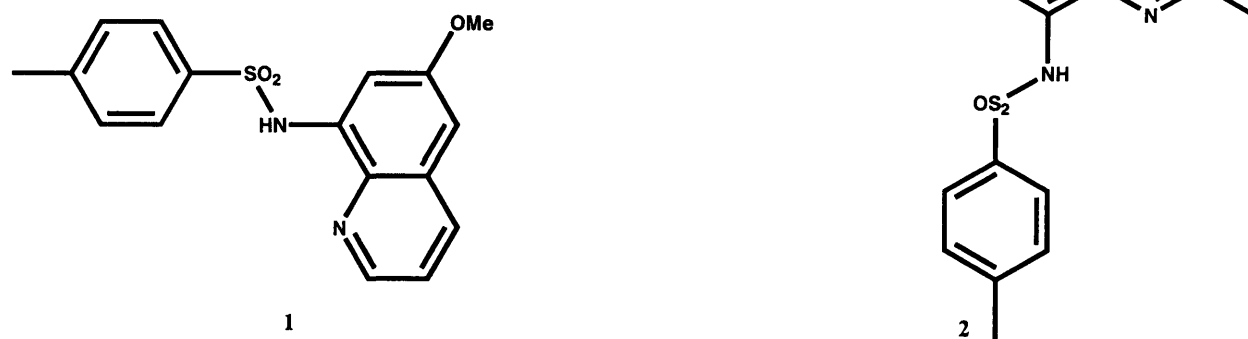


Figure 1: Early zinc sensors: TSQ (1)⁹ and Zinquin^{10,11} (2).

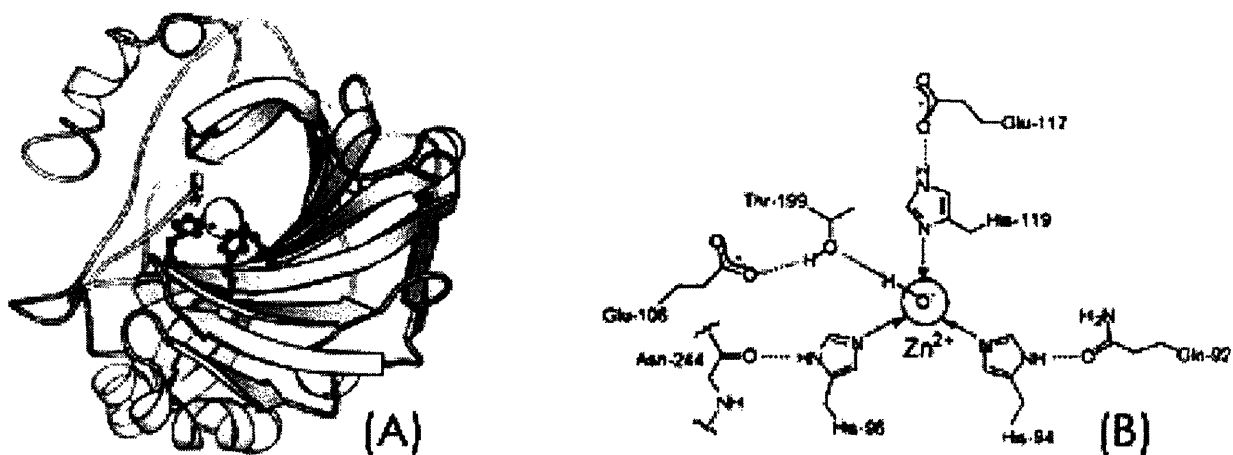


Figure 2: A High-Affinity Carbonic anhydrase-based Sensor.¹⁴
 (A) Ribbon diagram, (B) Its active site, which involves coordination by three imidazoles

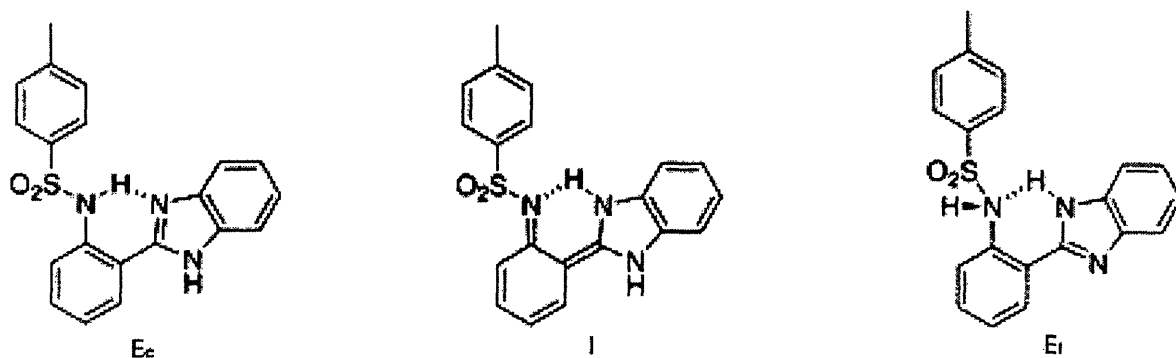


Figure 3: TPBI, a benzimidazole-based probe. Conversion from between cis (E_c) and trans (E_t) forms of enamines through rotation of the carbon-oxygen bond allows ESIPt to occur¹⁵

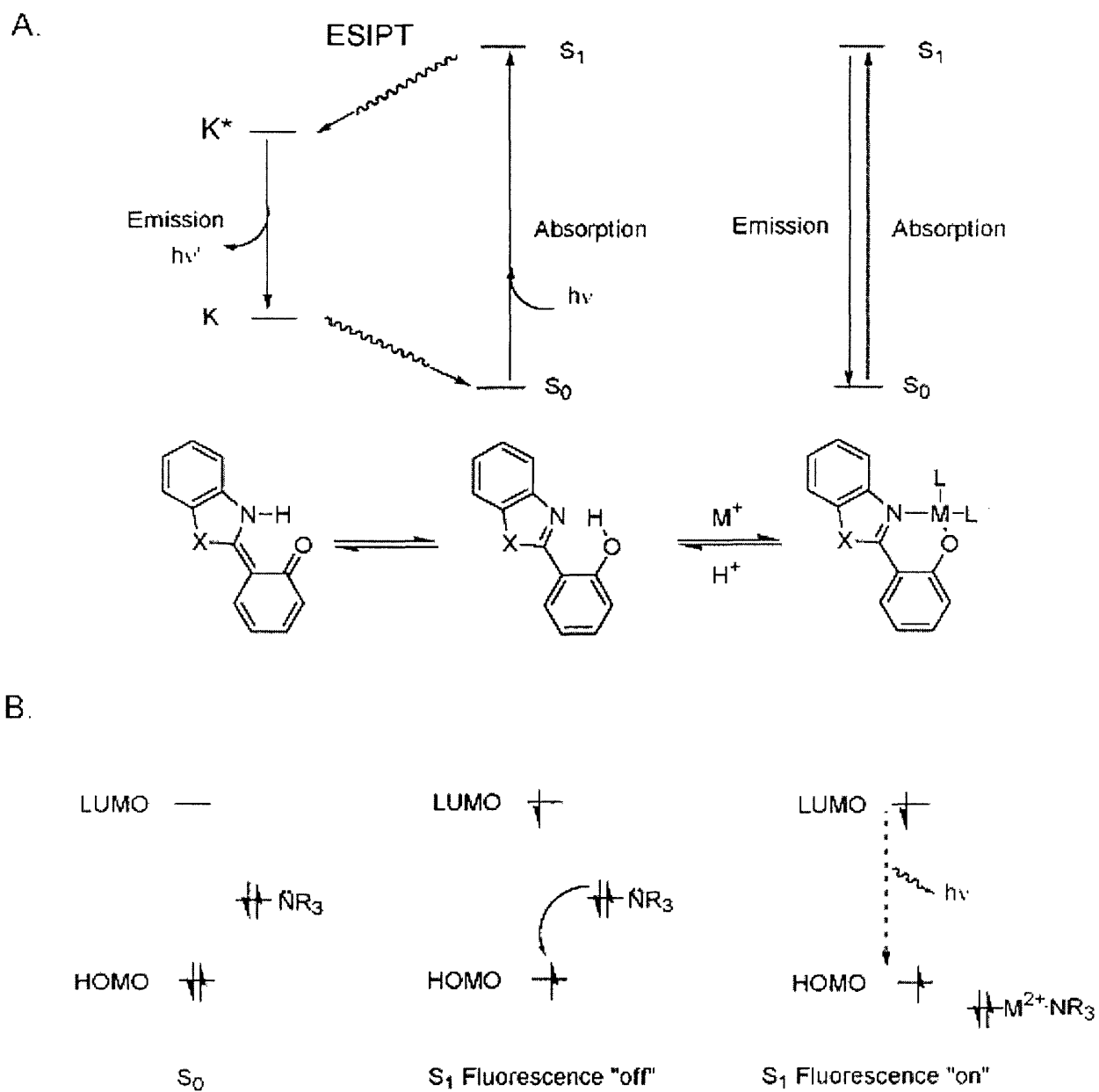
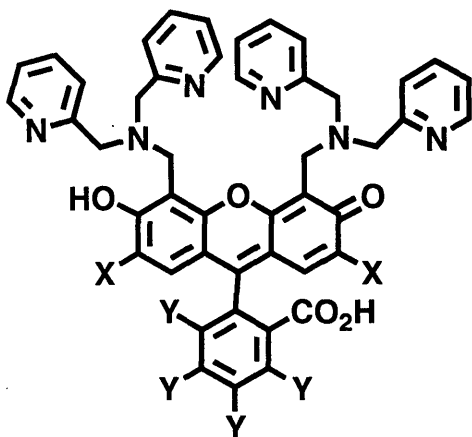
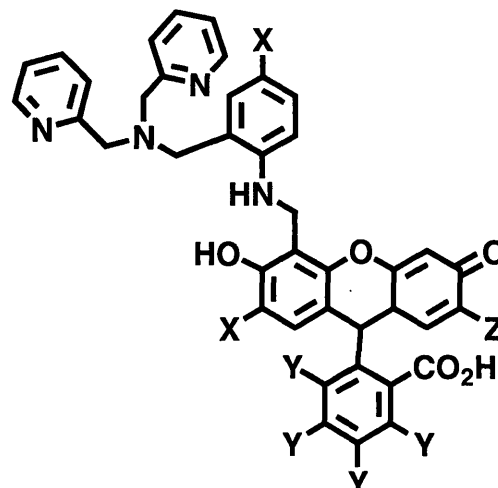


Figure 4: Mechanisms of ESIP¹⁵ (A) and PET (B)



- 3a: ZP1 (X = Cl, Y = H)
 3b: ZP2 (X = H, Y = H)
 3c: ZP3 (X = F, Y = H)
 3d: ZPF1 (X = Cl, Y = F)
 3e: ZPCl1 (X = Cl, Y = Cl)
 3f: ZPBr1 (X = Cl, Y = Br)
 3g: ZPF3 (X = F, Y = F)



- 4a: ZP4 (X = H, Y = H, Z = Cl)
 4b: ZP5 (X = F, Y = H, Z = Cl)
 4c: ZP6 (X = Cl, Y = H, Z = Cl)
 4d: ZP7 (X = OMe, Y = H, Z = Cl)
 4e: ZP8 (X = H, Y = F, Z = F)

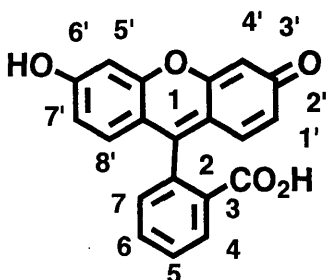


Figure 5: The Zinpyr (ZP) family of sensors and Nomenclature of Fluorescein (Parent Compound)

CHAPTER 2. An Esterase-Activated System for the Ratiometric Sensing of Biological Zinc

Esterase-Activated Two-Fluorophore System for Ratiometric Sensing of Biological Zinc(II)

Carolyn C. Woodroffe, Annie C. Won, and Stephen J. Lippard*

Department of Chemistry, Massachusetts Institute of Technology, Cambridge, Massachusetts 02139

Received August 31, 2004

Intracellular ester hydrolysis by cytosolic esterases is a common strategy used to trap fluorescent sensors within the cell. We have prepared analogues of Zinpyr-1 (ZP1), an intensity-based fluorescent sensor for Zn^{2+} , that are linked via an amido-ester or diester moiety to a calibrating fluorophore, coumarin 343. These compounds, designated Coumazin-1 and -2, are nonpolar and are quenched by intramolecular interactions between the two fluorophores. Esterase-catalyzed hydrolysis generates a Zn^{2+} -sensitive ZP1-like fluorophore and a Zn^{2+} -insensitive coumarin as a calibrating fluorophore. Upon excitation of the fluorophores, coumarin 343 emission relays information concerning sensor concentration whereas ZP1 emission indicates the relative concentration of Zn^{2+} -bound sensor. This approach enables intracellular monitoring of total sensor concentration and provides a ratiometric system for sensing biological zinc ion.

Introduction

Divalent zinc plays many important roles in biology.¹ Zn^{2+} is the second most abundant metal in the body and is a structural or catalytic component of more than 300 enzymes. Intracellular concentrations of free Zn^{2+} are closely controlled by a complex and effective system of zinc transporters and zinc-specific solute carriers,^{2,3} such that the free or loosely bound Zn^{2+} concentration in the cytosol is subfemtomolar.⁴ Much higher cytosolic concentrations of free Zn^{2+} are observed in cells that have undergone oxidative stress.⁵

The synaptic vesicles in the mossy fibers of mammalian hippocampus are of interest because accumulation of loosely bound Zn^{2+} , up to 0.3 mM in concentration, occurs in these intracellular compartments.^{6,7} An overriding justification for the entropic cost of this system has not been determined, in part because of the lack of an intrinsic spectroscopic signature with which to study Zn^{2+} and its physiological roles. The

development of fluorescent sensors for loosely bound Zn^{2+} is thus of interest in elucidating its movements and functions.

The application of fluorescent sensors to biological systems has traditionally been complicated by an inability to assess the local concentration of the probe. A localized bright fluorescent signal may reflect a large amount of analyte in that area, or it may be an artifact of high local dye concentration. Ratiometric sensors that display two distinctly different measurable signals in the presence and absence of analyte are thus of great interest and utility because they can eliminate such ambiguities.⁸

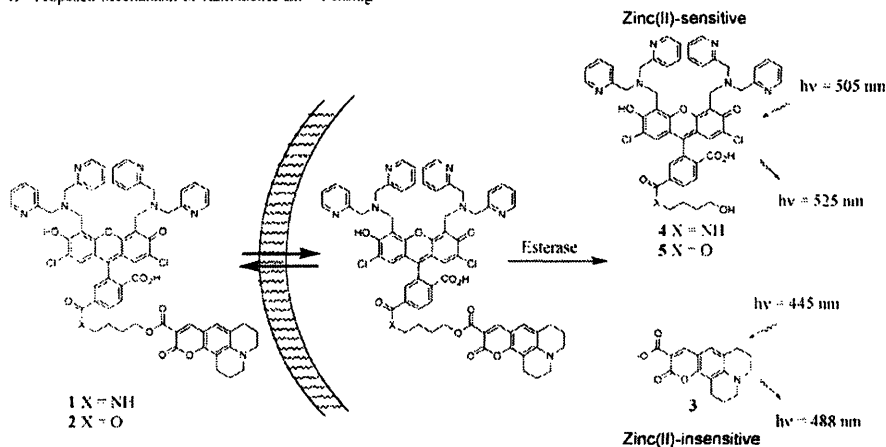
Several ratiometric fluorescent probes for biological zinc(II) ion have recently been described. The majority of these are based on fluorophores requiring relatively short-wavelength, high-energy excitation sources, such as 2-aryl benzimidazoles,⁹ benzoxazoles,¹⁰ and indoles and benzofurans.^{11,12} Binding of Zn^{2+} affords a wavelength shift in excitation or emission, based on interruption of fluorophore conjugation or on excited-state intramolecular proton transfer (ESIPT). Excitation wavelengths for these probes range from about 300 to 380 nm, and emission wavelengths vary

* To whom correspondence should be addressed. E-mail: lippard@mit.edu.

- (1) Vallee, B. L.; Falchuk, K. H. *Physiol. Rev.* **1993**, *73*, 79–118.
- (2) Palmieri, R. D.; Huang, L. *Pflügers Arch.—Eur. J. Physiol.* **2004**, *447*, 744–751.
- (3) Kambe, T.; Yamaguchi-Iwai, Y.; Sasaki, R.; Nagao, M. *Cell. Mol. Life Sci.* **2004**, *61*, 49–68.
- (4) Outten, C. E.; O'Halloran, T. V. *Science* **2001**, *292*, 2488–2492.
- (5) Chang, C. J.; Jaworski, J.; Nolan, E. M.; Sheng, M.; Lippard, S. J. *Proc. Natl. Acad. Sci. U.S.A.* **2004**, *101*, 1129–1134.
- (6) Frederickson, C. J. *Int. Rev. Neurobiol.* **1989**, *31*, 145–238.
- (7) Frederickson, C. J.; Suh, S. W.; Silva, D.; Frederickson, C. J.; Thompson, R. B. *J. Nutr.* **2000**, *130*, 1471S–1483S.

- (8) Tsien, R. Y.; Poenie, M. *Trends Biochem. Sci.* **1986**, *11*, 450–455.
- (9) Henary, M. M.; Wu, Y.; Fahrni, C. J. *Chem. Eur. J.* **2004**, *10*, 3015–3025.
- (10) Taki, M.; Wolford, J. L.; O'Halloran, T. V. *J. Am. Chem. Soc.* **2004**, *126*, 712–713.
- (11) Gee, K. R.; Zhou, Z. L.; Ton-That, D.; Sensi, S. L.; Weiss, J. H. *Cell Calcium* **2002**, *31*, 245–251.
- (12) Maruyama, S.; Kikuchi, K.; Hirano, I.; Urano, Y.; Nagano, T. *J. Am. Chem. Soc.* **2002**, *124*, 10650–10651.

Ratiometric Sensing of Biological Zinc(II)

Scheme 1. Proposed Mechanism of Ratiometric Zn^{2+} Sensing

between 395 and 532 nm. ZNP-1, a ratiometric probe with visible excitation, has recently been reported.⁵ A highly sensitive ($K_d < 10$ pM) carbonic-anhydrase-based zinc sensor that operates by a FRET mechanism is also available.¹³

We envisioned a ratiometric two-fluorophore sensing system in which a zinc-sensitive component was linked to a zinc-insensitive reporter in such a manner that the two would separate upon entering the cell. An ester-linked system seemed ideal for this application because carboxylate esterification is a common strategy in preparing cell-permeable, trappable sensors. The lipophilic esterified sensor can passively diffuse across the cell membrane, and once inside the cell the esters can be hydrolyzed by cytoplasmic esterases, regenerating the membrane-impermeant parent carboxylate 3 and compounds 4 and 5, which are expected to exhibit good intracellular retention.^{5,14–17} Scheme 1 illustrates the strategy.

The synthesis of ZPI species containing carboxylate functionalities on the bottom ring has been reported elsewhere.^{14,15} ZPI is a fluorescein-based Zn^{2+} sensor that is cell-permeable without prior modification,^{16,17} however, fluorescein-based compounds are typically membrane-impermeable owing to the predominance of a charged tautomer in aqueous solutions at neutral pH. Such fluorescein species are permeabilized by protecting the phenolic hydroxyl groups as hydrolytically labile acetates,¹⁸ trapping the fluorescein moiety in the cell-permeable lactone form.¹⁹ Esterification

of carboxylates with alkyl or functionalized alkyl groups is widely used for sensors in which the carboxylate is an integral part of the analyte-binding system or is introduced to increase solubility. Acetoxymethyl esters are particularly susceptible to hydrolysis,^{19,20} but ethyl esters^{9,21,22} are also commonly used, implying that simple alkyl esters are acceptable substrates for cytoplasmic esterases.

Coumarin-1 and -2 (CZ1, 1; CZ2, 2) are ZPI analogues containing coumarin 343 (3) as the reporter fluorophore bound via a hydrolyzable alkyl-amidoester or diester linker. Permeation of 1 or 2 into the cell and subsequent cleavage by intracellular esterases thus regenerates the parent fluorophores 3 and 4 or 5, enabling two-fluorophore ratiometric sensing of Zn^{2+} , as shown in Scheme 1. We report here the synthesis and physical characterization of these molecules as well as biological applications. A preliminary communication describing CZ1 has appeared previously.¹⁴

Experimental Section

Materials and Methods. Reagents were purchased from Aldrich and used without further purification except for coumarin 343, which was recrystallized from MeOH and CH_2Cl_2 before use. The pyridinium salt of 3',6'-diacetyl-2',7'-dichloro-6-carboxyfluorescein (6) was prepared as described.¹⁵ A porcine liver esterase (PLE) suspension was purchased from Sigma and used as supplied. SDS-PAGE gel analysis indicated the esterase solution to be a mixture of two major protein components, which we take as a crude estimate of what might be present in cells. The Michaelis–Menten constants reflect average values from PLE treatment. Acetonitrile and dichloromethane were obtained from a dry-still solvent dispensation system. Fluorescence spectra were acquired on a Hitachi F-3010 or a Photon Technology International (Lawrenceville, NJ) Quanta Master 4L-format scanning fluorimeter. The latter was equipped

- (13) Thompson, R. B.; Cramer, M. L.; Bozym, R.; Fierke, C. A. *J. Biomed. Opt.* **2002**, *7*, 555–560.
 (14) Woodrooffe, C. C.; Lippard, S. J. *J. Am. Chem. Soc.* **2003**, *125*, 11458–11459.
 (15) Woodrooffe, C. C.; Masalha, R.; Barnes, K. R.; Frederickson, C. J.; Lippard, S. J. *Chem. Biol.* **2004**, *11*, 1659–1666.
 (16) Walkup, G. K.; Burdette, S. C.; Lippard, S. J.; Tsien, R. Y. *J. Am. Chem. Soc.* **2000**, *122*, 5644–5645.
 (17) Burdette, S. C.; Walkup, G. K.; Spingler, B.; Tsien, R. Y.; Lippard, S. J. *J. Am. Chem. Soc.* **2001**, *123*, 7831–7841.
 (18) Adameczyk, M.; Chan, C. M.; Fino, J. R.; Mattingly, P. G. *J. Org. Chem.* **2000**, *65*, 596–601.
 (19) Haugland, R. P. *Handbook of Fluorescent Probes and Research Products*, Ninth Edition; Molecular Probes, Inc.: Eugene, OR, 2002.

- (20) Tsien, R. Y.; Pozzan, T.; Rink, T. J. *J. Cell Biol.* **1982**, *94*, 325–334.
 (21) Zalewski, P. D.; Millard, S. H.; Forbes, I. J.; Kapaniris, O.; Slavotinek, A.; Betts, W. H.; Ward, A. D.; Lincoln, S. F.; Maladevan, I. *J. Histochem. Cytochem.* **1994**, *42*, 877–884.
 (22) Nasir, M. S.; Fahrni, C. J.; Suhly, D. A.; Kolodtsick, K. J.; Singer, C. P.; O'Halloran, T. V. *J. Biol. Inorg. Chem.* **1999**, *4*, 775–783.

with an LPS-220B 75-W xenon lamp and power supply, an A-1010B lamp housing with integrated igniter, a switchable 814 photon-counting/analog PMT detector, and an MD-5020 motor driver. A Perkin-Elmer Analyst-300 atomic absorption spectrophotometer (AAS) with a Perkin-Elmer HGA-800 Graphite Furnace (GF-AAS) was used for atomic absorption (AA) spectroscopy measurements. UV-visible absorption spectra were recorded on a Cary 1E UV-visible spectrophotometer at 25 °C. Both were analyzed by using Kaleidagraph 3.0 for Windows. ¹H and ¹³C NMR spectra were acquired on a Varian 300 or 500 MHz or a Bruker 400 MHz spectrometer. High-resolution mass spectra were recorded on an FTMS electrospray apparatus by personnel at the MIT Department of Chemistry Instrumentation Facility. LCMS analysis was performed on an Agilent Technologies 1100 Series LCMS with a Zorbax Extend C-18 column using a linear gradient of 100% A (95:5 H₂O:MeCN, 0.05% HCO₂H) to 100% B (95:5 MeCN:H₂O; 0.05% HCO₂H) over 30 min at a flow rate of 0.250 mL/min. Detector wavelengths were set at 240 and 500 nm, and the MS detector was set to positive ion mode scanning the range *m/z* = 100–2000.

Synthetic Procedures. (a) *N*-(2-Hydroxyethyl)-3',6'-diacetyl-2',7'-dichlorofluorescein-6-amide (**9**). The pyridinium salt of 3',6'-diacetyl-2',7'-dichloro-6-carboxyfluorescein (**6**, 1.22 g, 2 mmol) was dissolved in dry CH₂Cl₂ containing 400 μL of DMF and stirred in a dry ice-acetone bath. Oxalyl chloride (1.5 mL, 2 M solution in CH₂Cl₂) was diluted with 25 mL of dry CH₂Cl₂ and added dropwise over 30 min. The reaction was stirred for an additional 30 min and then concentrated under reduced pressure. The resulting residue was dissolved in CH₂Cl₂. NaHCO₃ (336 mg, 4 mmol) was added, and the suspension was stirred at –78 °C as a solution of ethanolamine (390 μL, 409 mg, 6.6 mmol) in 15 mL of CH₂Cl₂ was added dropwise. The reaction was stirred overnight, at which time 40 mL of H₂O was added and the layers were separated. The aqueous layer was washed with 2 × 40 mL CH₂Cl₂; the combined organic layers were washed with saturated NaCl solution, dried over MgSO₄, and evaporated. The resulting residue was purified by flash chromatography on silica gel eluting with 98:2 → 96:4 CHCl₃:MeOH to give 450 mg (42%) of **9** as a colorless solid. ¹H NMR (CDCl₃): δ 8.10 (s, 2 H); 7.56 (s, 1 H); 7.11 (s, 2 H); 7.08 (t, 1 H); 6.84 (s, 1 H); 3.70 (t, 2 H); 3.49 (m, 2 H); 2.37 (s, 6 H). ¹³C NMR (CDCl₃): δ 168.40, 167.79, 166.32, 152.42, 149.72, 148.82, 141.52, 130.37, 129.15, 128.02, 126.27, 123.09, 122.53, 117.09, 113.04, 80.67, 61.79, 43.03, 20.82. mp 159–162 °C. HRMS (M + H): calcd for C₂₂H₂₀Cl₂NO₅: 572.0515; found 572.0529.

(b) **Mitsunobu Reaction of *N*-(2-Hydroxyethyl)-3',6'-diacetyl-2',7'-dichlorofluorescein-6-amide (**9**).** 55 mg, 0.1 mmol) was combined with coumarin 343 (29 mg, 0.1 mmol), triphenylphosphine (30 mg, 0.11 mmol), and DIAD (21 μL, 0.1 mmol) in dry CH₂Cl₂ and stirred 45 min at RT. The reaction was concentrated in vacuo, the residue was dissolved in minimal CH₂Cl₂, and Et₂O was added. The resulting orange crystalline solid was filtered off and one-half of the filtrate was loaded onto a preparative scale TLC plate. Compound **10** was isolated as the major product (17 mg, corresponds to 64% overall yield). ¹H NMR (CDCl₃): δ 8.28 (d, 1 H); 8.12 (d, 1 H); 7.76 (s, 1 H); 7.16 (s, 2 H); 6.87 (s, 2 H); 4.47 (t, 2 H); 4.08 (t, 2 H); 2.38 (s, 6 H). HRMS (M + Na): calcd for C₂₂H₂₀Cl₂NO₅Na: 576.0229; found 576.0216.

(c) **Coumarin 343 4-Hydroxybutyl Ester (**11**).** Coumarin 343 (3, 285 mg, 1 mmol) was combined with 4-benzyloxy-1-butanol (190 μL, 1.03 mmol), triphenylphosphine (280 mg, 1.07 mmol), and DIAD (210 μL, 1.01 mmol) in 20 mL of dry CH₂Cl₂. The reaction was stirred at RT for 90 min and then quenched with 20

mL of MeOH. Pd/C was added and the suspension was stirred under a H₂ atmosphere for 2 h, then filtered through Celite, and concentrated in vacuo. The viscous residue was purified by flash chromatography on silica gel eluting with 93:7 CHCl₃:MeOH and then crystallized from CHCl₃ layered with Et₂O. Filtration gave 277 mg of **11** (78% yield). ¹H NMR (CDCl₃): δ 8.36 (s, 1 H); 6.95 (s, 1 H); 4.35 (t, 2 H); 3.74 (t, 2 H); 3.34 (m, 4 H); 2.87 (t, 2 H); 2.77 (t, 2 H); 1.98 (m, 4 H); 1.75 (m, 4 H). ¹³C NMR (CDCl₃): δ 165.11, 159.20, 153.64, 149.76, 148.82, 127.19, 119.47, 107.76, 107.18, 105.82, 65.39, 62.06, 50.43, 50.04, 29.91, 27.57, 25.00, 21.27, 20.29, 20.18. mp 135–137 °C. HRMS (M + Na) calcd for C₂₀H₁₉NO₅Na: 380.1474; found 380.1463.

(d) **Coumarin 343 4-(6-Carboxy-3',6'-diacetyl-2',7'-dichlorofluorescein)butyl Ester (**12**).** Coumarin 343 4-hydroxybutyl ester (**11**, 268 mg, 0.75 mmol) was combined with 6-carboxy-2',7'-dichlorofluorescein-3',6'-diacetate pyridinium salt (479 mg, 0.78 mmol), triphenylphosphine (206 mg, 0.78 mmol), and DIAD (158 μL) in 30 mL of dry CH₂Cl₂ at RT and stirred overnight. More DIAD (79 μL) was then added. After 24 h the reaction was concentrated in vacuo and the desired product was isolated by flash chromatography on silica gel eluting with 98:2 → 90:10 CHCl₃:MeOH, followed by titration with MeOH to give 185 mg (28%) of **12**. ¹H NMR (CDCl₃): δ 8.38 (d, 1 H); 8.31 (s, 1 H); 8.14 (d, 1 H); 7.84 (s, 1 H); 7.18 (s, 2 H); 6.94 (s, 1 H); 6.85 (s, 2 H); 4.42 (t, 2 H); 4.35 (t, 2 H); 3.34 (m, 4 H); 2.88 (t, 2 H); 2.76 (t, 2 H); 2.38 (s, 6 H); 1.9–2.0 (m, 8 H). ¹³C NMR (CDCl₃): δ 168.08, 167.78, 164.88, 158.81, 153.70, 152.12, 149.86, 149.49, 148.85, 148.78, 137.57, 132.16, 129.17, 129.06, 127.18, 126.02, 125.39, 123.02, 119.37, 117.09, 113.11, 107.71, 107.38, 105.93, 80.95, 65.03, 64.44, 50.46, 50.07, 26.61, 24.60, 24.56, 21.33, 20.83, 20.35, 20.25. mp dec > 159 °C. HRMS (M + Na): calcd for C₄₂H₃₁Cl₂NO₇Na: 890.1383; found 890.1414.

(e) **Coumazin-2 (**2**).** Dipicolylamine (128 mg, 0.64 mmol) and paraformaldehyde (40 mg, 1.32 mmol) were combined in 10 mL of dry MeCN and heated to reflux for 45 min. A portion of **12** (87 mg, 0.1 mmol) was suspended in 5 mL of MeCN and added to the refluxing solution, followed by 5 mL of H₂O. The reaction was heated at reflux for 24 h, at which time it was cooled to RT, concentrated in vacuo, acidified with 5 drops of glacial acetic acid, and stored at 4 °C overnight. The resulting red precipitate was filtered to afford 87 mg (72%) of **2**. ¹H NMR (CDCl₃): δ 8.60 (d, 4 H); 8.38 (d, 2 H); 8.33 (s, 1 H); 8.10 (d, 1 H); 7.85 (s, 1 H); 7.67 (td, 4 H); 7.36 (d, 4 H); 7.20 (m, 4 H); 6.97 (s, 1 H); 6.60 (s, 2 H); 4.40 (t, 2 H); 4.32 (t, 2 H); 4.20 (s, 4 H); 4.01 (m, 8 H); 3.34 (m, 4 H); 2.86 (t, 2 H); 2.75 (t, 2 H); 1.80–1.98 (m, 12 H). mp dec > 151 °C. HRMS (M + H): calcd for C₇H₁₁Cl₂N₂O₁₁: 1206.3571; found 1206.3564.

(f) **6-Carboxy-2',7'-dichlorofluorescein-3',6'-diacetatesuccinimidyl Ester (**15**).** The pyridinium salt of 6-carboxy-2',7'-dichlorofluorescein-3',6'-diacetate (**6**, 945 mg, 1.5 mmol) was combined with 1-[3-(dimethylamino)propyl]-3-ethylcarbodiimide hydrochloride (EDC) (300 mg, 1.56 mmol) and *N*-hydroxysuccinimide (200 mg, 1.74 mmol) in 10 mL of 1:1 ethyl acetate:DMF and stirred at RT for 6 h. Brine (75 mL) and CH₂Cl₂ (50 mL) were added, and the layers were separated. The aqueous layer was extracted with 2 × 50 mL CH₂Cl₂, the combined organics were washed with 2 × 50 mL of 0.1 N HCl and 1 × 50 mL of brine, dried over MgSO₄, and evaporated. The resulting residue was purified by flash chromatography on silica gel eluting with 99:1 CHCl₃:MeOH to give 647 mg (0.48 mmol, 69%) of **15** as a glassy foam. ¹H NMR (CDCl₃): δ 8.44 (d, 1 H); 8.22 (d, 1 H); 7.93 (s, 1 H); 7.19 (s, 2 H); 6.84 (s, 2 H); 2.90 (dd, 4 H); 2.37 (s, 6 H). ¹³C NMR (CDCl₃): δ 168.90, 167.90, 167.00, 162.61, 160.43, 152.17, 149.62, 148.88,

Ratiometric Sensing of Biological Zinc(II)

132.72, 132.07, 130.66, 128.89, 126.30, 123.07, 116.36, 113.06, 80.84, 25.61, 20.67. mp 84–86 °C. HRMS (M + H): calcd for $C_{23}H_{18}Cl_2NO_4$: 626.0257; found 626.0220.

(g) *N*-(4-Hydroxybutyl)-2',7'-dichlorofluorescein-6-amide (16). 6-Carboxy-2',7'-dichlorofluorescein-3',6'-diacetate succinimidyl ester (15, 312 mg, 0.5 mmol) was dissolved in 1:1 CH_2Cl_2 :MeOH and stirred at RT with 4-aminobutanol (230 μ L, 222 mg, 2.5 mmol) overnight. The resulting red solution was concentrated on the rotary evaporator, taken up in 10 mL of H_2O , acidified with concentrated HCl, and filtered to afford an orange solid, which was dried overnight to give 235 mg of 16 (91% yield). 1H NMR (MeOH- d_4): δ 8.15 (s, 2 H); 7.62 (s, 1 H); 6.85 (s, 2 H); 6.68 (s, 2 H); 3.57 (t, 2 H); 3.35 (m, 2 H); 1.50–1.65 (m, 4 H). mp 179–180 °C (dec). HRMS (M – H): calcd for $C_{23}H_{18}Cl_2NO_5$: 514.0460; found 514.0474.

(h) ZPI(6-CONH(CH₂)₄OH) (4). Dipicolylamine (256 mg, 1.3 mmol) was combined with paraformaldehyde (36 mg, 2.6 mmol) in 10 mL of dry MeCN and heated to reflux for 45 min. *N*-(4-Hydroxybutyl)-2',7'-dichlorofluorescein-6-amide (103 mg, 0.2 mmol) was suspended in 15 mL of 1:1 MeCN:H₂O and added to the reaction, and reflux was continued for 24 h. The reaction was cooled to RT, acidified with 0.5 mL of glacial acetic acid, and concentrated under reduced pressure. The residue was diluted with MeOH and H₂O and stored at 4 °C overnight. Filtration afforded the desired product (19 mg, 10%). 1H NMR (MeOH- d_4): δ 8.53 (d, 4 H); 8.12 (s, 2 H); 7.63 (s, 1 H); 7.48 (d, 4 H); 7.30 (m, 4 H); 7.26 (t, 4 H); 6.67 (s, 2 H); 4.34 (s, 4 H); 4.18 (m, 8 H); 3.52 (t, 2 H); 3.37 (t, 2 H); 1.52–1.68 (m, 4 H). mp 157–159 °C (dec). HRMS (M + H): calcd for $C_{33}H_{46}Cl_2N_2O_7$: 938.2836; found 938.2843.

Spectroscopic Measurements. All glassware was washed sequentially with 20% HNO₃, deionized water, and ethanol before use. Purified water (resistivity 18.2 M Ω) was obtained from a Millipore Milli-Q water purification system. Fluorophore stock solutions in DMSO were made up to concentrations of 1 mM and kept at 4 °C in 100–500 μ L aliquots. Portions were thawed and diluted to the required concentrations immediately prior to each experiment. Fluorescence and absorption data were measured in HEPES buffer (50 mM, pH 7.5, KCl 100 mM) except for fluorometric pK_a titrations, which were performed in 100 mM KCl, pH 12.5, and for the fluorescein standard in quantum yield measurements, which was measured in 0.1 N NaOH. The HEPES buffer, prepared with Millipore water, contains 20 \pm 2 mg/L (0.3 \pm 0.03 μ M) of zinc as determined by flameless atomic absorption (AA) spectroscopy. Solutions were stored in clean, dry propylene containers and were filtered (0.25 μ m) before data acquisition. Fluorescence spectra were recorded from 425 to 650 nm. Extinction coefficients, quantum yields, fluorescence-dependent pK_a values, and dissociation constants were measured as previously described.¹⁴ All measurements were performed in triplicate.

(a) **Zn²⁺ Response of Esterase-Treated CZ Dyes.** A 10 mL portion of a 4 μ M solution of CZ1 in pH 7.5 HEPES buffer was incubated with a 10 μ L aliquot of PLE (10 mg/mL in 3.2 M (NH₄)₂SO₄) at RT for 12 h. A 2 mL aliquot was withdrawn and the fluorescence spectrum from 425 to 650 nm was acquired with excitation first at 445 nm and then at 505 nm. A 4 μ L aliquot of 10 mM ZnCl₂ was added and the fluorescence spectra were recorded as before. The procedure was repeated for CZ2 with incubation times varying from 1 to 6 h.

(b) **Michaelis–Menten Kinetics of Esterase Hydrolysis of CZ2.** A 5 μ L aliquot of PLE was added to a fluorescence cuvette containing 2 mL of pH 7.5 HEPES buffer and various concentrations (0.5 nM – 25 μ M) of CZ2. The cuvette was shaken vigorously and the emission intensity at 488 nm (excitation 445 nm) was

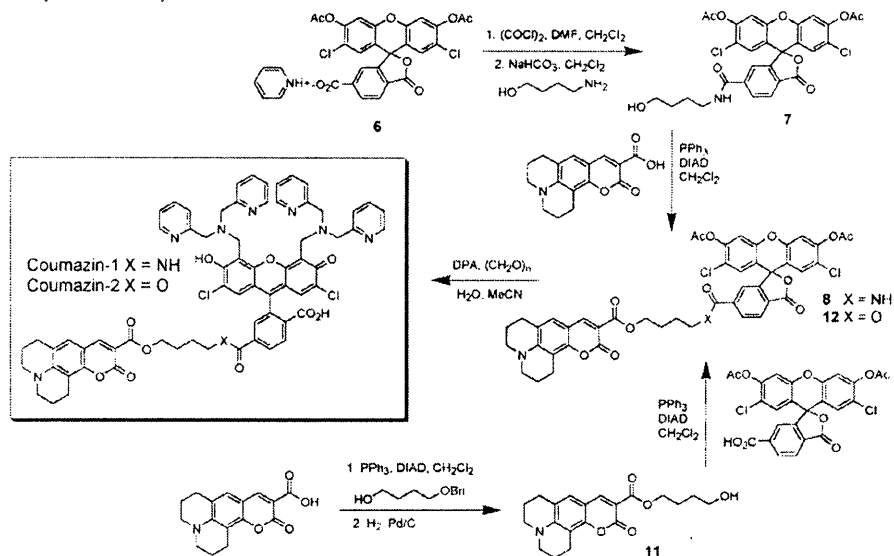
monitored for 5 min at 25 °C. The rate of increase in emission intensity between 100 and 200 s was determined and converted to μ mol/min of coumarin 343 produced using a standard curve. The rate of increase in concentration of coumarin 343 was plotted as a function of substrate concentration and fit by using a Michaelis–Menten model.

(c) **LCMS Determination of CZ1 and CZ2 Ester Hydrolysis Products.** A 10 μ M solution of CZ1 (20 μ L of a 1 mM DMSO stock solution of CZ1 and 5 μ L PLE suspension in 2 mL HEPES buffer (50 mM, pH 7.5)) was incubated 19 h at 22 °C in a polystyrene tube covered with aluminum foil, filtered, and analyzed by LCMS. The major peaks observed were at 10.8 min (no assignable mass), 13.0 min (m/z = 469.9), and 18.4 min (m/z = 593.1). A 10 μ M solution of CZ2 was similarly prepared and incubated for 1 h before LCMS analysis. The major peaks observed were at 14.8 min (m/z = 939.2) and 18.1 min (m/z = 593.1). Retention times were determined for 10 μ M standard solutions of expected metabolites for comparison and were as follows: 3 18.5 min (m/z = 593.1; calcd for 2M + Na = 593.2); 4 12.9 min (m/z = 469.2; calcd for (M + 2H)²⁺ = 469.2); 11 17.2 min (m/z = 380.3; calcd for M + Na = 380.2).

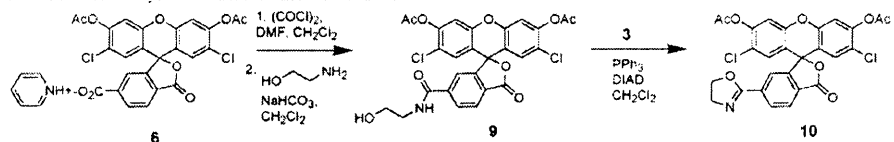
(d) **Absorption Spectroscopy of PLE-Treated CZ1 and CZ2.** A 20 μ L aliquot of 1 mM CZ1 stock solution (DMSO) was added to 2 mL of HEPES buffer. A 10 μ L aliquot of PLE suspension was added, and the absorbance spectrum was acquired periodically over 6 h. The procedure was repeated for CZ2.

Imaging. HeLa cells were grown at 37 °C under a 5% CO₂ atmosphere in Dulbecco's modified Eagle's medium (DMEM, Gibco/BRL) supplemented with 10% fetal bovine serum, 1x penicillin/streptomycin, and 2 mM L-glutamine. Coumazin-1 and Coumazin-2 were stable in EMEM and DMEM over 4 h at 37 °C under conditions used for cell studies, as monitored by fluorescence at both excitation wavelengths (445 or 505 nm). Cells were plated 24 h before study into 2 mL imaging dishes. Cells were approximately 50% confluent at the time of study. A 20 μ L aliquot of dye (1 mM DMSO) was added to each 2 mL dish, and the cells were incubated for 4 h at 37 °C, at which point the medium was aspirated and the cells were washed twice with phosphate-buffered saline solution (PBS), resuspended in dye-free EMEM (Mediatech), and examined on a Zeiss Axiovert 200M inverted epifluorescence microscope with a 40 \times oil immersion, a mercury lamp light source, and differential interference contrast (DIC), operated by OpenLab software (Improvision, Lexington, MA). Samples were maintained at 37 °C over the course of the imaging experiment. The amount of zinc in the cell growth medium was 20 \pm 2 μ g/L (0.3 \pm 0.03 μ M) and 60 \pm 2 μ g/L (0.9 \pm 0.03 μ M) for DMEM and EMEM, respectively, as determined by flameless AA spectroscopy. Images were collected at 30 s intervals for 30 min during the course of the experiment, as a 10 μ L aliquot of a solution containing 1 μ M ZnCl₂ and 9 μ M sodium pyruvate was added. The fluorescence response reached a maximum at about 10–15 min after addition of ZnCl₂, at which time a 10 μ L aliquot of 10 μ M TPEN was added. At each time point, four images were collected in rapid succession: a DIC image (775DF50 emission) and three fluorescence images using a CFP filter (420DF20 excitation, 450DRLP dichroic, 475DF40 emission), a FRET filter (420DF20 excitation, 450DRLP dichroic, 530DR30 emission), and a YFP filter (495DF10 excitation, 515DRLP dichroic, 530DF30 emission). Fluorescence images were background-corrected. Acquisition times were in the range of 100–250 ms. A control experiment in which a 10 μ L aliquot of 10 μ M TPEN was added to the imaging dish without prior addition of exogenous ZnCl₂ was performed using a similar protocol.

Scheme 2. Synthesis of CZ Dyes



Scheme 3. Intramolecular Cyclization under Mitsunobu Conditions



Results and Discussion

Synthesis. The compounds Coumazin-1 and -2 were synthesized as shown in Scheme 2. The choice of an *n*-butyl linker in the synthesis of CZ1¹⁴ was not arbitrary. Our initial approach involved the hydroxyethylamide **9**; however, the Mitsunobu condensation conditions gave primarily the intramolecular cyclization product **10**, as shown in Scheme 3. Oxazole formation of β -hydroxyethyl amides under Mitsunobu conditions is well precedented in the literature,^{23–25} notably in syntheses of paclitaxel and related compounds. Similar problems were encountered with a propyl linker (data not shown). The butyl linker would form a thermodynamically unfavorable seven-membered ring as the product of such an intramolecular condensation, allowing the desired intermolecular reaction to dominate.

The approach to Coumazin-2 (CZ2) was slightly different. Mitsunobu condensation of coumarin 343 with 4-benzyloxyl-1-butanol followed by hydrogenation furnished the coumarin hydroxybutyl ester **11** in 78% yield over two steps. Removal of the diisopropyl hydrazidodicarboxylate byproduct from the intermediate benzyl ether was extremely difficult and

reduced the overall yield; hence, the most expedient route was to carry the undesired byproduct through and remove it from the deprotected **11** by crystallization. A second Mitsunobu reaction of **11** with the diacetyldichlorofluorescein carboxylate **6** was sluggish, proceeding only to 28% conversion. The reaction yield was not improved by using the free acid of the fluorescein moiety rather than the pyridinium salt. The resulting diester-linked fluorescein-coumarin compound **12** was subjected to standard Mannich conditions and furnished the desired coumpound CZ2 (**2**) in 72% yield.

The expected ZP hydrolysis product **4** of CZ1 was synthesized as shown in Scheme 4. Determination of the photophysical and thermodynamic properties of **4** confirmed that the extension of the alkyl chain by two methylene units does not noticeably alter the fluorescence properties or Zn²⁺ response of **4** as compared with the previously reported analogue **13**. Oxalyl chloride activation was employed in the synthesis of **13**; however, this reaction was sensitive to a variety of experimental factors and the extent of conversion to the acid chloride was somewhat variable, leading to mixtures that included deprotected starting material. Alternative methods of activation were therefore sought. EDC-mediated coupling of **6** to *N*-hydroxysuccinimide proceeded in reasonable yield to give the succinimidyl ester **15**, an activated intermediate that can be purified by column chromatography. Subsequent reaction with a 3-fold or greater

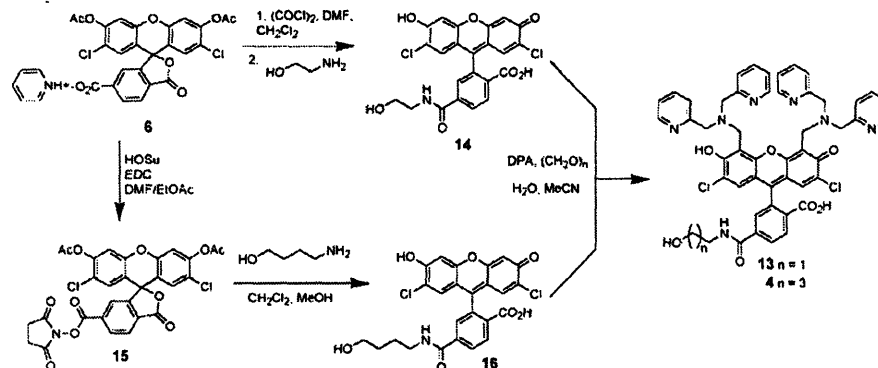
(23) Hamamoto, H.; Mamedov, V. A.; Kitamoto, M.; Hayashi, N.; Tsuboi, S. *Tetrahedron: Asymmetry* **2000**, *11*, 4485–4497.

(24) Cevallos, A.; Rus, R.; Moyano, A.; Pericas, M. A.; Riera, A. *Tetrahedron: Asymmetry* **2000**, *11*, 4407–4416.

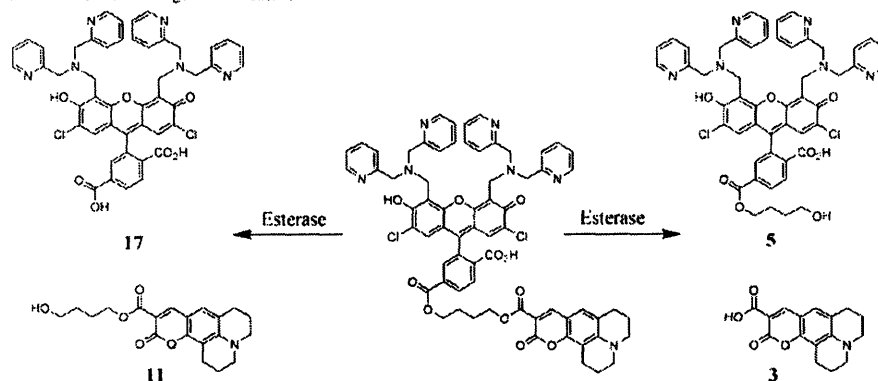
(25) Mandar, I.; Kuroda, A.; Okumoto, H.; Nakanishi, K.; Mikuni, K.; Hara, K.; Hara, K. *Tetrahedron Lett* **1999**, *41*, 243–246.

Ratiometric Sensing of Biological Zinc(II)

Scheme 4. Synthesis of Putative ZP1 Metabolites



Scheme 5. Possible Esterase Digestion Products of CZ2



excess of amine in mixed $\text{CH}_2\text{Cl}_2/\text{MeOH}$ yielded the deprotected fluoresceinamide **16**, which can be isolated by simple precipitation after removal of organic solvents, providing a straightforward and practical route to simple fluoresceinamides. Subsequent Mannich reaction of **14** furnished the desired amide-substituted ZP1 adduct **4**. Extinction coefficients and quantum yields for **4** with and without Zn^{2+} were measured, and the dissociation constants and fluorescence response of **4** to Zn^{2+} are essentially identical to those of the previously reported **13**.¹⁴ CZ2 contains two possible sites for ester hydrolysis. Esterase digestion can therefore produce ZP1 hydroxybutyl ester **5** or ZP1(6- CO_2H) (**17**), as shown in Scheme 5. The Zn^{2+} -sensing properties of ester- or acid-functionalized ZP1 carboxylates have been described elsewhere.¹³ Measured constants for putative CZ fragments or analogues thereof are listed in Table 1. All of these ZP1-like hydrolysis products may be expected to function effectively as Zn^{2+} sensors.

Photophysics and Thermodynamics. The photophysical properties of CZ1 and CZ2 have been examined, and relevant data are listed in Table 1. Both coumarin compounds fluoresce extremely weakly prior to esterase processing, regardless of the fluorophore excited. Whereas a Förster resonance energy transfer (FRET) mechanism might account

Table 1. Photochemical Properties of CZ Dyes and Their Expected Cleavage Fragments

	ϵ ($\text{M}^{-1}\text{cm}^{-1}$)	λ_{max} (nm) absorbance	Φ_{ZP1}	Φ_{coumarin}	K_d (nM)	pK _a
4	62000	519	0.22		0.25	—
4 + Zn^{2+}	65000	509	0.69			
13	71100	518	0.21		0.20	8.43
13 + Zn^{2+}	78600	508	0.67			
17 ^a	76000	516	0.21		0.16	7.12
17 + Zn^{2+}	81000	506	0.63			
ZP1-6- CO_2Et ^b	61000	519	0.13		0.37	7.00
+ Zn^{2+}	72000	509	0.67			
CZ1 ^a	37200	451	0.02	0.01	0.25	
	38600	526				
CZ1 + Zn^{2+}	41000	449	0.04	0.01		
	38100	518				
CZ2	26000	450	0.02	0.01		
	22400	526				
CZ2 + Zn^{2+}	26567	448	0.04	0.01		
	24333	521				

^a Data reproduced from ref 14 for comparison purposes. ^b Data reproduced from ref 15.

for quenching of the putative donor, such a process would require a concomitant increase in the fluorescence emission of the putative acceptor, which is not observed. ZP1 fluorescence in both cases is similarly quenched, implying that the Förster interaction is not the major mechanism of

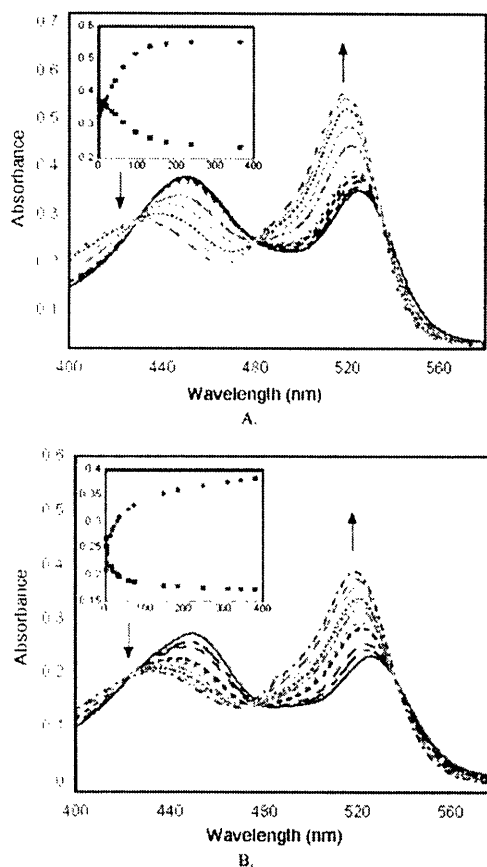


Figure 1. Time-dependent changes in absorption spectra for CZ1 over 6 h (A) and CZ2 over 3 h (B) upon treatment with porcine liver esterase. Insets: changes in absorption at 519 nm (red circles) and 450 nm (blue squares) as a function of time (min).

quenching.²⁰ In addition, the extinction coefficients of CZ1 and CZ2 are significantly reduced in comparison to their ZP counterparts (Table 1). Treatment of either CZ1 or CZ2 with porcine liver esterase (PLE) effects an increase in intensity of nearly 100% and a blue shift from 526 to 519 nm in the absorption band corresponding to the ZP1 absorbance (Figure 1). The coumarin absorption band similarly undergoes a blue shift from 450 to 435 nm, but the intensity of the band decreases by approximately 40%. The lack of a perfectly clean isosbestic point at 480 nm for CZ2 compared to CZ1 may indicate multiple reactions, possibly because of the potential for hydrolysis at two sites. This extreme change signals a strong interaction between fluorophores and is further evidence that the Förster mechanism, a weak interaction that requires little to no alteration in the absorption

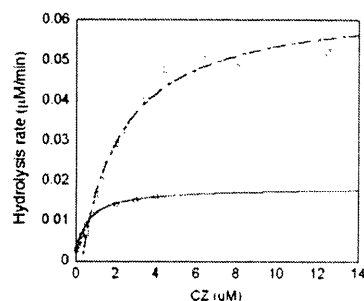


Figure 2. Michaelis–Menten fit of the CZ esterase hydrolysis rate. CZ1 (red circles) was treated with 75 nM PLE, and CZ2 (blue squares) was treated with 37.5 nM PLE. For both compounds, measurements were made at 25 °C in HEPES buffer (pH 7.5). Hydrolysis rate was assumed to be the rate of production of coumarin 343, determined by using a standard curve.

Table 2. Michaelis–Menten Constants for CZ Dyes

	k_{cat} (min^{-1})	k_{cat}/K_M ($\mu\text{M}^{-1} \text{min}^{-1}$)
CZ1	0.017	0.027
CZ2	0.211	0.128

spectrum, is probably not operative.²⁷ Other reports of such extreme quenching in the case of covalently linked FRET-capable fluorophores, combined with significant changes in the absorption spectrum, have been accounted for by excitation theory,^{26,28} and such may be the case here. Quantum yields determined over a 0.1–2.0 μM range were identical within experimental error, indicating no contribution of intermolecular quenching to the mechanism.

The kinetics of PLE action on both compounds were assayed fluorimetrically (Figure 2), revealing that, like the changes in the absorption spectrum, the fluorescence increases much more rapidly for CZ2 than for CZ1. Hydrolysis of either ester in CZ2 will afford roughly the same fluorescence increase. Similarly, after the first hydrolysis event for each CZ2 molecule, the second hydrolysis event will show no fluorescence response but may act as a competing substrate. Although the Michaelis–Menten constants (Table 2) measured for CZ2 are valid for comparison of the fluorescence response with values measured for CZ1, the fluorescence response may arise from more than one reaction and the reported values are therefore considered to be only rough approximations. Nonetheless, hydrolysis of CZ2 is clearly much more efficient than hydrolysis of CZ1, with significantly greater pseudo- k_{cat} (12.4-fold) and pseudo- k_{cat}/K_M (4.7-fold) values (Table 2). Such a large effect cannot be explained by the statistical presence of twice as many substrates and was initially attributed to greater activity of PLE on the ZP1 ester compared to the coumarin ester. To examine this possibility, the CZ2 PLE cleavage products were analyzed by LCMS after 1 h of incubation. The major peaks observed appeared with retention times of 14.8 min (m/z (M + H) = 939.2) and 18.1 min (m/z (2M + H) +

(26) Packard, B. Z.; Toptygin, D. D.; Komoriya, A.; Brand, L. *Biophys Chem.* 1997, 67, 167–176.

(27) Foerster, T. In *Modern Quantum Chemistry*; Sinanoglu, O., Ed.; Academic Press: New York, 1965; Vol. 3, pp 99–137.

(28) Packard, B. Z.; Toptygin, D. D.; Komoriya, A.; Brand, L. *Proc Natl Acad. Sci. U.S.A.* 1996, 93, 11640–11645.

Ratiometric Sensing of Biological Zinc(II)

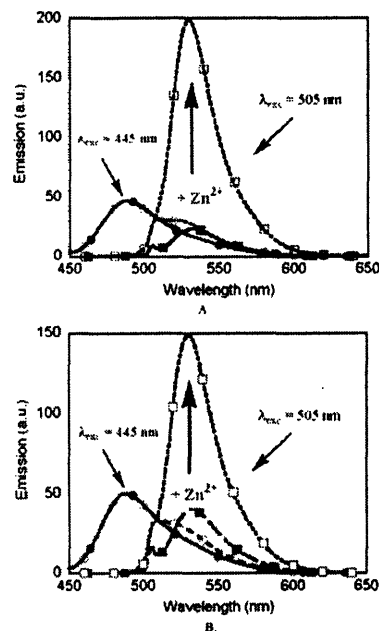


Figure 3. Fluorescence response of esterase-treated CZ1 (A) and CZ2 (B). Aliquots (10 mL) of HEPES buffer containing 2 μ M dye were treated with porcine liver esterase for 19 h (CZ1, A) or 4 h (CZ2, B) and emission spectra were recorded with excitation at 445 nm (red solid circles) and 505 nm (blue solid squares). A 10 μ M portion of ZnCl₂ was added, and emission spectra were again recorded with excitation at 445 nm (green open circles) and 505 nm (black open squares).

Na)/2 = 593.1), corresponding to 5 and 3, respectively. These products are expected from hydrolysis at the coumarin ester (Scheme 4). Since no peak or signal for 17 could be observed during a standard run, its absence in the CZ2 product mix is not conclusive. However, the lack of detectable amounts of the complementary product 11, which gives a clear signal at 17.2 min ($m/z(M + Na) = 380.3$) when run in a control, is strong circumstantial evidence that the coumarin ester is cleaved first with good selectivity. Thus, the increase in rate of hydrolysis appears to stem primarily from enhanced activity of the enzyme on 2 over 1. LCMS analysis of CZ1 after 19 h exposure to PLE showed products of hydrolysis at the single ester functionality, as expected (4, 13.0 min, $(M + 2H) = 469.9$ and 3, 18.4 min, $(2M + Na) = 593.1$).

The fluorescence responses of esterase-treated CZ1 and CZ2 were also examined. As expected, excitation at 445 nm afforded coumarin fluorescence at 490 nm, and the coumarin emission spectrum was largely unaltered upon addition of excess ZnCl₂. Calibration curves of zinc chloride addition to CZ1 and CZ2 reveal a linear response for excitation at 505 nm and none when the excitation wavelength was 445 nm (Figures S1 and S2, Supporting Information). Some ZP1 fluorescence at 535 nm is observed for both compounds and increases significantly after addition of Zn²⁺. This contribution can be excluded by measuring fluorescence intensity at 488 nm or by instituting a cutoff of 500 nm in measuring

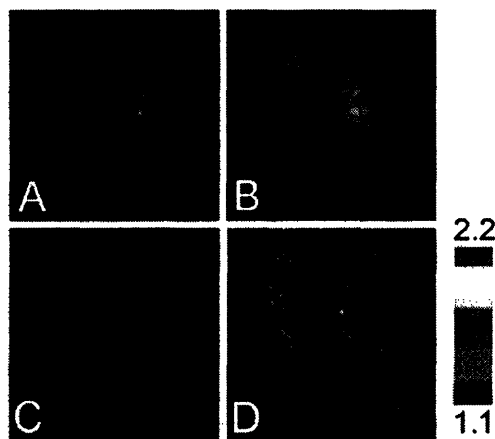


Figure 4. Fluorescence ratio images of HeLa cells treated with CZ2 after addition of ZnCl₂ and sodium pyrithione (A, 0 min; B, 8 min), and after subsequent treatment with TPEN (C, 8 min). D: DIC image. Images were acquired at 40 \times magnification, and the faux-color ratio range was 1.1 (blue)–2.2 (red).

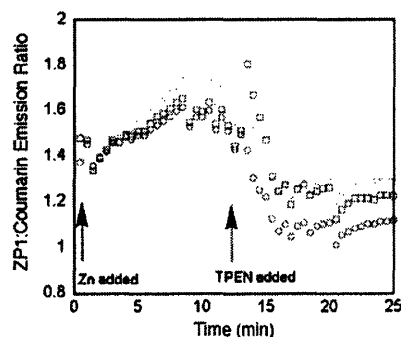


Figure 5. Intensity ratios of ZP1 emission divided by coumarin emission as a function of time. Three separate regions of interest were defined at the start of the experiment and total integrated emission of ZP1 divided by integrated emission of coumarin 343 was measured at 30 s intervals. ZnCl₂ (5 μ M final concentration) and sodium pyrithione (45 μ M) were added at 5 min, and TPEN (50 μ M) was added at 17 min.

integrated fluorescence emission area for coumarin. This ZP1 emission band arises from the ability of fluorescein to absorb some photons even when excited at 445 nm. Excitation at 505 nm affords a classic ZP1 emission band, which increases several-fold in response to addition of ZnCl₂. Surprisingly, addition of saturating ZnCl₂ to esterase-treated CZ2 results in only a 4-fold increase in the ratio of ZP1 integrated emission to coumarin 343 integrated emission compared with the ratio in the absence of Zn²⁺, whereas an 8-fold increase is observed for CZ1 (Figure 3). The ratio of ZP1:coumarin fluorescence for CZ2 remains relatively constant over several hours.

Biological Imaging. HeLa cells were stained by addition of an aliquot of 1 mM CZ2 in DMSO, to give a final concentration of 10 mM dye in the medium. After incubation for 4 h, the cells were washed and resuspended in dye-free

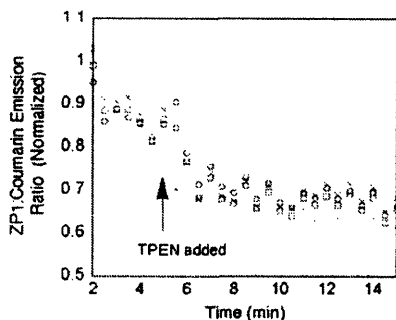


Figure 6. TPEN decreases intensity ratios of ZP1 emission divided by coumarin emission in CZ2-stained HeLa cells without exogenously added zinc. Four separate regions of interest were defined at the start of the experiment and total integrated emission of ZP1 divided by integrated emission of coumarin 343 was measured at 30 s intervals. TPEN (50 μ M) was added at 5 min.

medium, and the area immediately surrounding the site of application was imaged (Figure 4). The introduction of ZnCl₂-sodium pyrithione resulted in a hyperbolic increase in ZP1 emission over approximately 10 min with no change in coumarin emission (Figure 5). TPEN was added after ZP1 emission had reached an apparent maximum, and the ZP1 emission decreased to slightly lower than initial levels. Coumarin emission was not affected throughout the experiment. The intracellular distribution of the two dyes appears to be reasonably consistent, as assessed by the images after treatment with zinc-pyrithione and after treatment with TPEN. Both dyes are concentrated in the perinuclear area, and relatively good colocalization is observed, based on the Zn²⁺- and TPEN-treated images (Figure 4B,C). An exception to this general observation is an oval-shaped area in each cell, which displays slightly different intensity ratios compared to its surroundings and probably corresponds to the cell nucleus. This result may arise from different partitioning of the nuclear membrane by the ZP1 and coumarin hydrolysis

products, with a corresponding difference in fluorescence ratios. The TPEN-induced decrease in the ZP1:coumarin fluorescence ratio to values below the initial levels probably reflects the presence of some Zn²⁺-bound dye before exogenous zinc ion and the ionophore are added, because addition of TPEN to CZ2-treated cells without prior addition of Zn²⁺ and pyrithione also decreased the intensity ratio, as shown in Figure 6.

Summary and Conclusions

We describe a new approach to ratiometric sensing of intracellular Zn²⁺ based on the well-known phenomenon of intracellular hydrolysis of esterases. The compounds CZ1 and CZ2 are based on ZP1 sensors linked to the Zn²⁺-insensitive reporter fluorophore coumarin 343 by an amide-ester or diester moiety. The CZ compounds have very low fluorescence, but upon treatment with porcine liver esterase the ZP1-based Zn²⁺ sensor and reporter fluorophore fluorescence is regenerated. CZ2 is activated more rapidly than CZ1, although the same ester moiety is hydrolyzed first in both cases. CZ2 has been applied to image exogenous Zn²⁺ in HeLa cells and displays an increase in fluorescence ratio upon treatment with Zn²⁺ and an ionophore. The fluorescence ratio decreases below initial levels upon treatment with TPEN, a result in accord with other recent reports.¹⁰

Acknowledgment. This work was supported by the NIGMS under Grant GM65519. We thank Professor A. Y. Ting and Mr. C.-W. Lin for help in using their epifluorescence microscope. HeLa cells were provided by Mrs. K. R. Barnes and Ms. C. Saouma.

Supporting Information Available: Figures S1 and S2 displaying the fluorescence response of CZ1 and CZ2 over a zinc concentration range following excitation at 445 or 505 nm. This material is available free of charge via the Internet at <http://pubs.acs.org>.

IC0487895

Supporting Information for
Esterase-Activated Two-Fluorophore System for Ratiometric Sensing of Biological
Zinc(II)

Carolyn C. Woodroffe, Annie C. Won, and Stephen J. Lippard*
Contribution from the Department of Chemistry, Massachusetts Institute of Technology,
Cambridge, MA 02139

Figure Captions

Figure S1: Post-hydrolytic fluorescence response of 2 μ M CZ1 to zinc(II) chloride in HEPES buffer (see Experimental Section) when excited at the coumarin (445 nm) or fluorescein (505 nm) wavelength. The zinc-induced response maximizes at slightly less than 1:1 stoichiometry since no attempt was made to remove zinc impurities that are known to exist in the buffer (A. G. Tennyson and S. J. Lippard, unpublished results).

Figure S2: Post-hydrolytic fluorescence response of 2 μ M CZ2 to zinc(II) chloride in HEPES buffer (see Experimental Section) when excited at the coumarin (445 nm) or fluorescein (505 nm) wavelength. The zinc-induced response maximizes at slightly less than 1:1 stoichiometry since no attempt was made to remove zinc impurities that are known to exist in the buffer (A. G. Tennyson and S. J. Lippard, unpublished results).

Figure S1

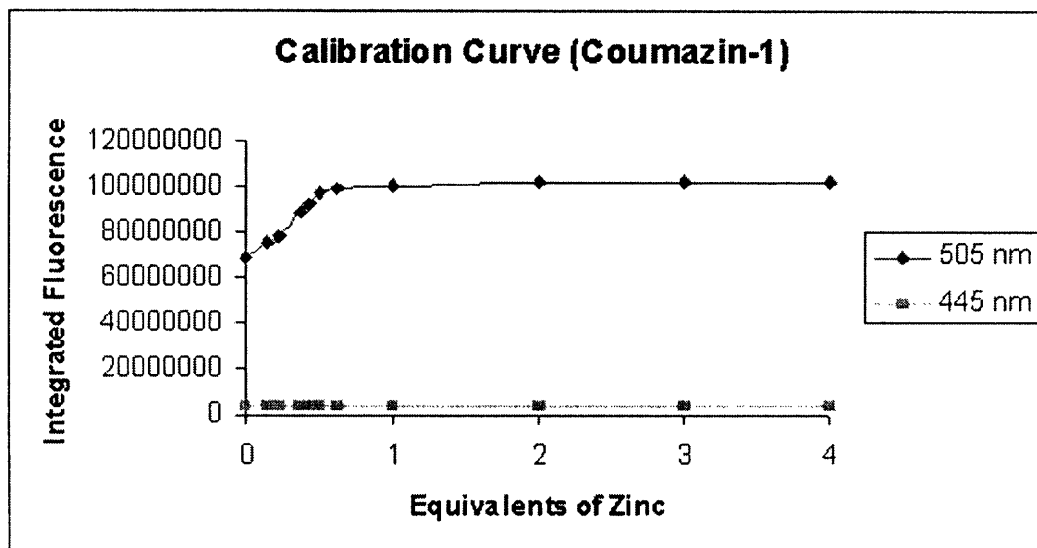
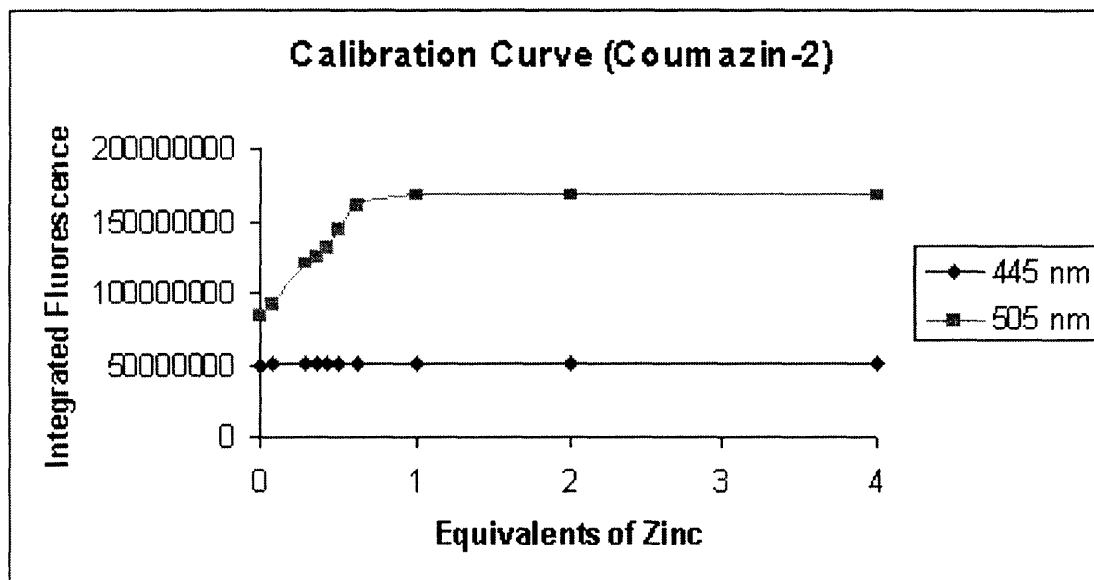


Figure S2



CHAPTER 3: Syntheses of Zinpyr Derivatives for Localized Applications in Zn²⁺ Sensing

CHAPTER 3: Syntheses of Zinpyr Derivatives for Localized Applications in Zn²⁺ Sensing

Introduction

Two strategies have been developed for the sensing of biological zinc in specific cell regions and receptor sites. Recent interest has sprung regarding the role of extracellular zinc inhibition in N-methyl-D-aspartate (NMDA) receptors.¹ NMDA receptors have been found to be involved in not only neuronal development and synaptic plasticity,² and in neurological disorders and neurodegeneration.³ Elucidation of the role of Zn²⁺ in NMDA-R inhibition may provide some insight regarding the role of NMDA receptors in the above processes and disorders.⁴ Current methods of studying NMDA receptors involve the excitation of hippocampal slices and subsequent monitoring of zinc release. Unfortunately, the synaptic cleft is narrow, making it difficult for these methods to provide specific information regarding the activity and concentrations of synaptically released zinc.⁵

Zinpyr-1 sensors functionalized with NMDA antagonists can bind to the NMDA receptor, and the coupled products could be used to monitor Zn²⁺ concentrations and activity in synaptic regions. Since many NMDA antagonists are functionalized with amines, we have investigated Zinpyr derivatives that couple directly to these moieties.

As demonstrated in Chapter 2, succinimidyl esters react readily with amines to create stable amide linkages. We therefore aimed to synthesize and isolate a Zinpyr-5-carboxy-succinimidyl ester (ZPOSu) intermediate, which can be coupled to diaminopimelic acid, a commercially available NMDA antagonist. After the coupled products are synthesized, they can be used in cell studies to label the NMDA receptor and monitor zinc flux at the receptor channels.

¹ Koh JY, Suh SW, Gwag BJ, He YY, Hsu CY, Choi, DW. *Science* **1996**, 272, 1013-1016

² McBain CJ, Mayer ML *Physiol Rev.* **1994**, 74, 723-760

³ Choi DW. *Science* **1992**, 258, 241-243

⁴ Peters S, Koh J, Choi DW *Science* **1987**, 236, 589-593

⁵ Assaf, SY, Chung SH *Nature* **1984**, 308, 734-738

An additional approach involves the use of Zinpyr derivatives that couple to small peptides for intracellular applications. The RGD peptide localizes to epithelial cells and has been selected because of its commercial availability and facile synthesis. Recent developments in click chemistry⁶ have suggested that a Zinpyr alkyne and an azide-functionalized peptide may be readily coupled with this method. Preparation of an azido amino acid has been demonstrated in the literature, by combining α -amino acids with a triflyl azide reagent.⁷ An azido-RGD peptide could be similarly prepared. A Zinpyr alkyne (**2**) has been synthesized, as an orthogonal click chemistry substrate.

Synthesis

We have tried several routes to synthesize a Zinpyr succinimidyl ester (ZPOSu), and have found that the reaction of **4** with disuccinimidyl carbonate in the presence of Et₃N and 6:1 MeCN/DMF achieves ZPOSu (**5**) in 52% yield (Figure 2). Compound **5** is a good activated intermediate and couples readily to diaminopimelic acid to give **6**. This preparation demonstrates that ZPOSu can be used to readily couple to other primary amine-containing NMDA antagonists. It should be noted that care must be taken with the isolated ZPOSu intermediate to avoid decomposition; ZPOSu should be stored under anhydrous, inert conditions, to avoid hydrolysis to the Zinpyr acid.

A Zinpyr alkyne (Figure 1) (**2**) and an azide-functionalized RGD peptide (**7**) have been investigated as potential click chemistry substrates. Click chemistry methods have been developed by Sharpless, *et al*,⁸ to create 1,4-triazoles stereoselectively from the 1,3-dipolar cycloaddition of alkynes and azides. These reactions involve a Cu(I) catalyst generated by the *in*

⁶ Hartmuth C. Kolb, Dr., Finn, M. G., Sharpless, K. *Barry. Angewandte Chemie International Edition* **2000**, 40(11), 2004-2021

⁷ Rijkers, D. T. S.; van Vugt, R.; Jacobs, H. J. F.; Liskamp, R. M. J. *Tet Lett* **2002**, 43, 3657-3660

⁸ Hartmuth C. Kolb, Dr., Finn, M. G., Sharpless, K. *Barry. Angewandte Chemie International Edition* **2000**, 40(11), 2004-2021

situ reduction of a Cu(II) salt (such as $\text{CuSO}_4 \cdot 5\text{H}_2\text{O}$). Click chemistry reactions are generally very high-yielding, ranging from 90-100%. Compound **2** has been synthesized and couples readily to an alkyl azide⁹ to generate **3** (Figure 1). Due to the fact that **3** binds the copper catalyst more strongly than it binds zinc, products were treated with Chelex resin to remove residual copper.

Compound **8** is generated by coupling an RGD azide (**7**) to **2** under click chemistry conditions. This azide-functionalized peptide can be generated by addition of a triflyl azide reagent to the RGD peptide, which selectively transforms its N-terminal α -amino group into an azide (Figure 1).⁷ To functionalize the RGD peptide with an azide group, triflyl azide is synthesized and added to the resin-bound RGD peptide. Non-resin-bound products were isolated by treatment with a 95% trifluoroacetic acid (TFA) solution. The Zinpyr alkyne was then added under click chemistry conditions in a 1:1 mixture of MeOH/H₂O, to produce a copper-containing product. Chelex is added to remove copper. Unfortunately, LCMS analysis shows no evidence of Zinpyr-RGD coupled product, before or after Chelex resin addition. This is probably due to the presence of residual TFA, from triflyl azide synthesis; TFA may have caused decomposition of the Zinpyr alkyne to its parent fluorescein compound.

Conclusions

Syntheses of Zinpyr-RGD coupled products have failed. One explanation for this is that the triflyl azide reaction may not have worked. It is also possible that traces of strong acid, specifically TFA, used in the synthesis of triflyl azide, may have caused Zinpyr decomposition, before click chemistry coupling could occur. To avoid decomposition of the Zinpyr moiety, the

⁹ Badiang, J.; Aubé, J. *J. Org. Chem.* **1996**, 61(7) 2484-57

triflyl azide solution should be neutralized before attempting the synthesis of a Zinpyr-RGD coupled product.

The Zinpyr alkyne has been synthesized and found to be an effective click chemistry substrate. Under Sharpless conditions, the alkyne effectively couples to an alkyl azide. Copper-free products have been isolated in low (10%) yield. After click-chemistry coupling, the resulting residue is treated with Chelex in dichloromethane (DCM) to remove residual copper from the Zinpyr moiety. Unfortunately, the coupled products are minimally soluble in DCM. After filtration, the Chelex was fluorescent, when illuminated with a UV lamp, indicating that some Zinpyr-containing product had not been isolated in dichloromethane. The copper-containing products are somewhat soluble in methanol; however, MeOH also dissolves the Chelex resin, making the isolation of copper-free products more difficult. Centrifugation and dialysis methods will be investigated to facilitate isolation of coupled products.

A Zinpyr succinimidyl ester (**4**) has been synthesized in decent yield. Coupling of the isolated ZPOSu with diaminopimelic acid affords a single adduct (**5**) that is easily isolated by preparative HPLC. It is probably more facile to react the succinimidyl ester intermediate directly with a diamine, followed by purification. This alternative, involving no direct isolation of the ZPOSu intermediate, may occur in fewer steps with better overall yields.

Experimental

Materials and Methods.

Reagents were purchased from Aldrich and used without further purification, except for pyBOP, which was obtained from NovaBiochem, and Chelex resin, which was obtained from Sigma. Azidopropanol was prepared as previously described.¹⁰ 3',6'-Diacetyl-2',7'-dichloro-6-

carboxyfluorescein pyridinium salt and ZP1(6-CO₂H) (**5**) were synthesized as described in Chapter 2. Acetonitrile was obtained from a dry-still solvent dispensation system. ¹H NMR and ¹³C spectra were acquired on a Bruker 400 MHz or a Varian 500 MHz spectrometer. LCMS analysis was performed on an Agilent Technologies 1100 Series LCMS with a Zorbax Extend C-18 column using a linear gradient of 100% A (95:5 H₂O:MeCN, 0.05% HCO₂H) to 100% B (95:5 MeCN:H₂O; 0.05% HCO₂H) over 30 min at a flow rate of 0.250 mL/min. Detector wavelengths were set at 240 nm and 500 nm, and the electrospray MS detector was set to positive ion mode scanning the range m/z = 100-2000. Low-resolution MS spectra were acquired on the same instrument. Preparative high-performance liquid chromatography (HPLC) was performed on a Waters 600 pump with a Waters 600E systems controller monitored by a Waters 486 tunable absorbance detector, using a Higgins Analytical, Inc. reverse-phase C18 column measuring 250 mm x 20 mm. Solvents A and B were purified water (resistivity 18.2 Ohms) obtained from a Millipore Milli-Q water purification system, or low-water acetonitrile (Mallinckrodt), respectively, each containing 0.1 % v/v trifluoroacetic acid. Isolated compounds were stored at 4 °C or -25 °C. The Zinpyr acid (**4**) was prepared as described in Chapter 2.

Synthetic Procedures

3',6'-Diacetyl-6-carboxy-2',7'-dichlorofluorescein propargylamide (1). 3',6'-Diacetyl-2',7',-dichlorofluorescein-6-carboxyfluorescein pyridinium salt (0.524 g, 1 mmol), pyBOP (0.781 g, 1.5 mmol), triethylamine (0.140 mL, 1 mmol), and propargylamine (0.110 g, 2 mmol) were dissolved in dry dichloromethane and stirred at room temperature for two hours. The solution was then washed with water (1x100 mL), 0.1M HCl (1x100 mL), and saturated NaCl (1x100 mL), dried over MgSO₄, and concentrated. The reaction was then purified by flash chromatography, eluting with 98:2 chloroform:methanol, to give 0.327 g (58%) of light yellow

foam. $^1\text{H NMR}$ (CDCl_3): δ 8.2 (q, 2H); 7.6 (s, 1H); 7.2 (s, 2H); 6.9 (s, 2H); 6.4 (t, 1H); 4.2 (m, 2H); 2.4 (s, 6H); 2.3 (t, 1H). HRMS(M-H): Calcd for $\text{C}_{28}\text{H}_{16}\text{Cl}_2\text{NO}_8$: 564.0253; Found 564.0242.

ZP1-6-(CONHCH₂CCH) (2). Di-(2-picolyl)amine (DPA) (0.23 mL, 1.3 mmol) and paraformaldehyde (0.256 g, 2.6 mmol) were added to dry acetonitrile and heated to reflux for forty-five minutes. Compound 1 (0.113 g, 0.2 mmol) was added in 10 mL acetonitrile and 10 mL H₂O, and refluxing continued for 24 h. The reaction was then concentrated, 10 mL H₂O and about 15 mL acetonitrile were added, after which light pink precipitate formation was observed. The reaction was allowed to stand at RT overnight and then filtered to give 0.074 g (41%) of light pink solid. $^1\text{H NMR}$ ($\text{DMSO}-d_6$): δ 9.2 (t, 2H); 4H (m, 4H); 8.1 (d, 1H); 8 (d, 1H); 7.8 (t, 4H); 7.7 (s, 1H); 7.4 (d, 4H); 7.3 (d, 4H); 6.6 (s, 2H); 4.2 (s, 2H); 4.0 (s, 4H); 3.4 (s, 8H), 3.1 (s, 1H). Calcd for $\text{C}_{50}\text{H}_{40}\text{Cl}_2\text{N}_7\text{O}_6$: 904.2417; Found 904.2435.

N-[1-(3-hydroxy-propyl)-1H-[1,2,3]triazol-4-ylmethyl]-ZP1-6-carboxamide (3). Compound (2) (0.010 g, 0.011 mmol), $\text{CuSO}_4 \cdot 5\text{H}_2\text{O}$ (0.003 g, 0.011 mmol), sodium ascorbate (0.022 g in 0.022 mL H₂O, 0.11 mmol), and azidopropanol (0.002 g, 0.022 mmol) were added to a 6 mL of 1:1 H₂O/MeOH. The reaction was stirred at RT for 24 hours, after which it was concentrated and lyophilized. LCMS analysis ($[\text{M} + 2\text{Cu}^{2+} - 2\text{H}^+]/2$): calculated 566.6; observed 565.2) revealed that no starting material remained, and that copper was bound to both Zinpyr binding sites. To remove the copper, the reaction was stirred vigorously in dichloromethane for two hours with Chelex (1 g), gravity filtered, and concentrated on the rotary evaporator to yield a pink residue (0.001 g, 10%). $^1\text{H NMR}$ (CDCl_3): 8.6 (d, 4H); 8.1 (d, 2H); 8.6 (t, 4H); 8.6 (s, 1H);

7.4 (d, 4H); 7.2 (t, 4H); 6.6 (s, 2H); 4.2 (s, 4H); 4.0 (s, 8H); 3.8 (t, 4H);* 3.6 (t, 4H);* 3.5 (t, 4H);* 3.5 (t, 4H); 3.5 (s, 1H);* 3.4 (t, 6H);* 1.9 (m, 6H).* (* = residual azide)

ZP1-6-CO₂Su (5). ZP1(6-CO₂H) (**4**) (86.6 mg, 0.1 mmol) was combined with disuccinimidyl dicarbonate (52.5 mg, 0.2 mmol), activated molecular sieves, and triethylamine (160 μ L) in 3 mL of DMF and 15 mL of MeCN. The reaction was stirred for 48 h at RT, and then concentrated under reduced pressure and quenched by addition of glacial AcOH. The product was isolated by preparative HPLC eluting with a gradient of 0 \rightarrow 100% B over 30 min. The peak eluting at 19 min was collected and the combined fractions were lyophilized to afford 50.2 mg (52% yield). Remaining starting material (18 mg, 21%) was also recovered (retention time: 16.8 min). ¹H NMR (MeOH-d₄): δ 8.62 (d, 4 H); 8.51 (dd, 1 H); 8.40 (d, 1 H); 7.96 (td, 4 H); 7.90 (d, 1 H); 7.42-7.55 (m, 8 H); 6.75 (s, 2 H); 4.49-4.58 (m, 12 H); 2.90 (br s, 4 H). MS(M + H): Calc. for C₅₁H₄₀Cl₂N₇O₉: 964.2; Found 964.3.

ZP1-Diaminopimelic Acid (6). ZP1-6-CO₂Su (**5**) (9.6 mg, 0.01 mmol) was dissolved in 0.5 mL of DMF and added to a solution of diaminopimelic acid (38.0 mg, 0.20 mmol) and triethylamine (30 μ L) in 3 mL of H₂O. The reaction was stirred for 2 h at RT, then quenched by addition of 20 μ L of glacial acetic acid. The desired product was isolated by preparative HPLC eluting with a gradient of 0 \rightarrow 100% B over 35 min. Lyophilization afforded 2.5 mg (37.6%) of a pink solid. ¹H NMR (MeOH-d₄): δ 8.63 (d, 4 H); 8.31 (d, 1 H); 8.22 (d, 1 H); 7.97 (m, 4 H); 7.66 (s, 1 H); 7.41-7.54 (m, 9 H); 6.73 (s, 1 H); 6.69 (s, 1 H); 4.57 (m, 1 H); 4.48-4.56 (m, 12 H); 3.96 (m, 1 H); 1.89-2.06 (m, 4 H); 1.65 (m, 2 H). MS(M+H): Calc. for C₅₄H₄₈Cl₂N₈O₁₀: 1039.3; Found 1039.2.

Click Chemistry Coupling of the ZP alkyne and RGD peptide (8). Sodium azide (0.0013 g, 0.02 mmol) is suspended in 1.5 mL water at 0 °C. 2.5 mL of dichloromethane is added, and the solution is stirred vigorously. Triflic anhydride (7 μ L, 0.04 mmol) is added in 2 mL dichloromethane over five minutes in an addition funnel. The reaction mixture is stirred at 0 °C for 2 h, and then washed with two 1.25 mL portions of dichloromethane. Organic layers are combined and dried over MgSO_4 .

Resin-bound RGD peptide (20 mg, 0.01 mmol) is dissolved in 0.1 mL water. Triethylamine (2.1 μ L, 0.015 mmol), $\text{CuSO}_4 \cdot 5\text{H}_2\text{O}$ (0.0024 g, 0.015 mmol), 0.1 mL MeOH, 0.9 mL dichloromethane, and the triflyl azide solution (0.01 mmol) are added. The reaction is stirred for 18 h, concentrated on the rotary evaporator, washed with MeOH and dichloromethane, and stirred in a 5 mL solution of 95% TFA, 2.5% TIPS, and 2.5% water (to remove the resin). The solution is then filtered, the filtrate is concentrated, and cold diethyl ether is added to form a dark brown precipitate. The Zinpyr alkyne (**2**) (0.010 g, 0.011 mmol), sodium ascorbate (0.0218 g, 0.1 mmol), $\text{CuSO}_4 \cdot 5\text{H}_2\text{O}$ (0.0002g, 0.011 mmol) is then added in 6 mL of a 1:1 solution of MeOH:water. The reaction is stirred vigorously for 24 hours, diluted with water, and cooled on ice. The solution is filtered, and the precipitate is washed with cold water and air dried overnight.

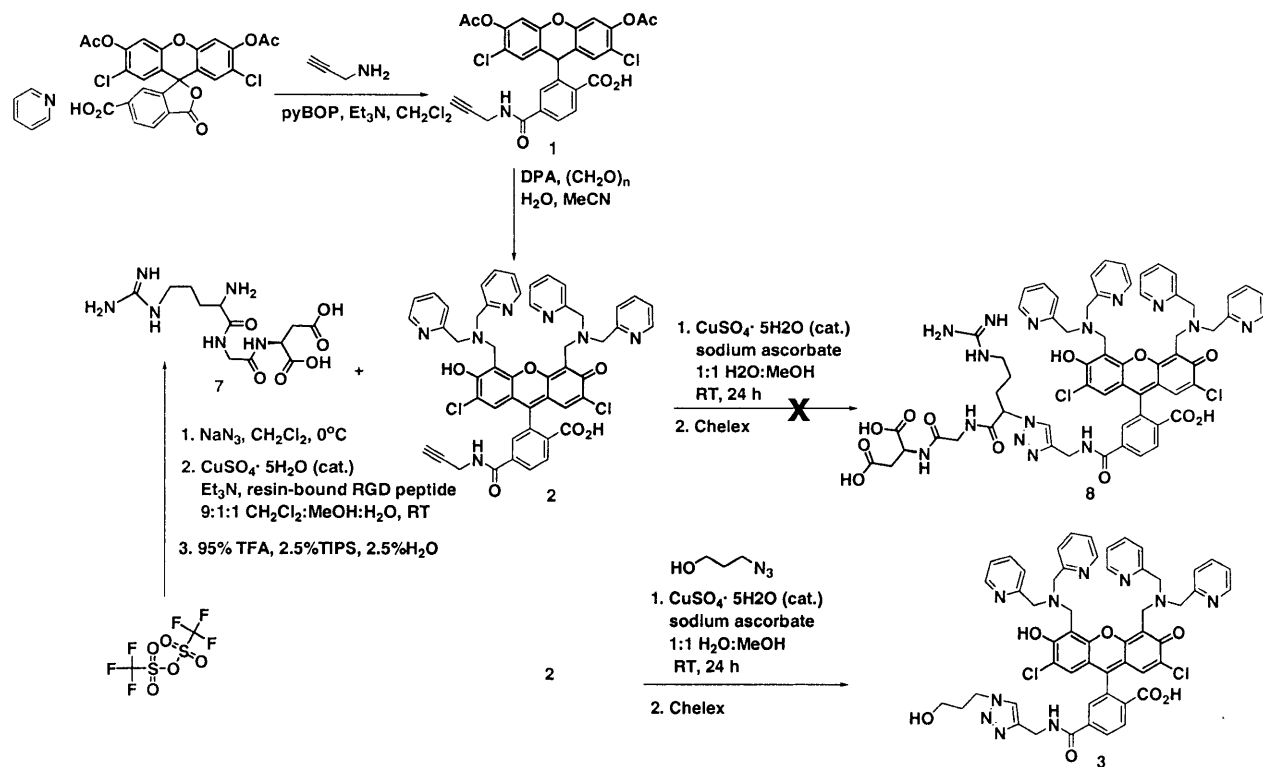


Figure 1: Synthesis of ZP1 Alkyne and its click chemistry reactions with azidopropanol and RGD azide

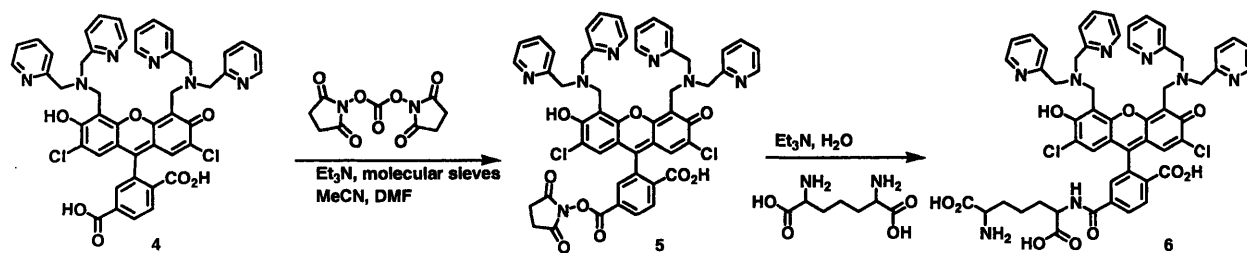


Figure 2: Reaction of the Zinpyr succinimidyl ester with diaminopimelic acid

CHAPTER 4: Conjugated Polymers as Nitric Oxide Sensors

Chapter 4: Conjugated Polymers as Nitric Oxide Sensors

Introduction

Since its identification as the endothelium-derived relaxing factor in biological systems, much interest in nitric oxide (NO) has been generated.¹ Nitric oxide is a small neutral free radical with one unpaired electron and acts as a messenger molecule in the nervous, immune, and cardiovascular systems.^{2, 3} NO is a neurotransmitter⁴ and plays central roles in memory formation and learning, as well as zinc release in neurons.⁵ Much controversy surrounds the role of NO in cancer and metastasis;⁶ conflicting studies suggest that NO may either contribute to or defend against metastases.⁷ Further evidence suggests that NO is also involved in apoptosis and necrosis⁸. Biological NO is produced in the body by the nitric oxide synthase-mediated oxidation of L-arginine to L-citrulline and NO. There are three general forms of NOS: endothelial NOS (eNOS), neuronal NOS (nNOS), and inducible NOS (iNOS).⁹ Endothelial NOS and neuronal

¹ Ignarro, L. J.; Buga, G. M.; Byrns, R. E.; Wood, K. S.; Chaudhuri, G. *J. Pharm. Exper. Therapeutics* **1998**, *246*, 218-26

² a) Ignarro, L. J. *Angew. Chem., Int. Ed.* **1999**, *38*, 1882-1892. b) Furchgott, R. F. *Angew. Chem., Int. Ed.* **1999**, *38*, 1870-1880. c) Murad, F. *Angew. Chem., Int. Ed.* **1999**, *38*, 1856-1868.

³ a) McCleverty, J. A. *Chem. Rev.* **2004**, *104*, 403-418. b) Moncada, S.; Higgs, E. A. *Eur. J. Clin. Invest.* **1991**, *21*, 361-74. c) Moncada, S.; Palmer, R. M.; Higgs, E. A. *Pharm. Rev.* **1991**, *43*, 109-42.

⁴ (a) Dugas, N.; Delfraissy, J.-F.; Tardieu, M. *Res. Immun.* **1995**, *146*, 707-10. (b) Egberongbe, Y. I.; Gentleman, S. M.; Falkai, P.; Bogerts, B.; Polak, J. M.; Roberts, G. W. *Neuroscience* **1994**, *59*, 561-78. (c) Huang, E. P. *Curr. Biol.* **1997**, *7*, R141-143. (d) Yamada, K.; Nabeshima, T. *Curr. Top. Pharm.* **1998**, *4*, 77-86.

⁵ (a) Berendji, D.; Kolb-Bachofen, V.; Meyer, K. L.; Grapenthin, O.; Weber, H.; Wahn, V.; Kroncke, K.-D. *FEBS Lett.* **1997**, *405*, 37-41. (b) Kroncke, K. D.; Fehsel, K.; Schmidt, T.; Zenke, F. T.; Dasting, I.; Wesener, J. R.; Bettermann, H.; Breunig, K. D.; Kolbbachoffen, V. *Biochem. Biophys. Res. Commun.* **1994**, *200*, 1105-1110.

⁶ (a) Alexandrova, R.; Mileva, M.; Zvetkova, E. *Exper. Path. Parasit.* **2001**, *4*, 13-18. (b) Wink, D. A.; Mitchell, J. B. *Free Rad. Biol. Med.* **2003**, *34*, 951-954. (c) Buga, G. M.; Ignarro, L. J. *Nitric Oxide* **2000**, 895-920. (d) Mooschala, S.; Rajnakova, A. *Free Rad. Res.* **1999**, *31*, 671-679. (e) Wink, D. A.; Vodovotz, Y.; Laval, F.; Dewhirst, M. W.; Mitchell, J. B. *Carcinogenesis* **1998**, *19*, 711-721.

⁷ Lala, P. K. *Cancer and Metastasis Revs.* **1998**, *17*, 1-6.

⁸ (a) Xie, K.; Huang, S. *Free Rad. Biol. Med.* **2003**, *34*, 969-986. (b) Bal-Price, A.; Brown, G. C. *J. Neurochem.* **2000**, *75*, 1455-1464.

⁹ (a) Fischmann, T. O.; Hruza, A.; Niu, X. D.; Fossetta, J. D.; Lunn, C. A.; Dolphin, E.; Prongay, A. J.; Reichert, P.; Lundell, D. J.; Narula, S. K.; Weber, P. C. *Nature Struct. Biol.* **1999**, *6*, 233-242. (b) Charles, I. G.; Palmer, R. M.; Hickery, M. S.; Bayliss, M. T.; Chubb, A. P.; Hall, V. S.; Moss, D. W.; Moncada, S. *Proc. Nat. Acad. Sci.* **1993**, *90*, 11419-23. (c) Garvey, E. P.; Tuttle, J. V.; Covington, K.; Merrill, B. M.; Wood, E. R.; Baylis, S. A.; Charles, I. G. *Arch Biochem. Biophys.* **1994**, *311*, 235-41. (d) Wang, Y.; Marsden, P. A. *Curr. Op. Nephrol. Hypertension* **1995**, *4*, 12-22.

NOS produce low concentrations of NO after activation by calcium and calmodulin.¹⁰ Higher concentrations of NO can occur if a cytokine activates iNOS.¹¹

Current NO sensing techniques, such as EPR, chemiluminescence, and the use of microelectrodes, generally involve irreversible reactions and indirect measurements. Recent efforts have focused on the development of fluorescent NO sensors which can provide accurate, quantitative and direct measurements. Previously developed fluorescent sensors include solid-bound fiber optic-based probes which have specific, micromolar affinity for NO. Unfortunately, these sensors react with other forms of NO, such as NO⁺, and often produce irreproducible results, due to tedious multi-step fabrication techniques.¹²

The Lippard lab has developed several fluorescent NO sensors.¹³ Transition metal complexes have been synthesized with coordinated fluorophores (Figure 1). These complexes react reversibly with NO; in the presence of NO, the fluorophore dissociates from the coordination sphere of the metal. A metal nitrosyl complex is formed, and the displaced fluorophore is no longer quenched. Careful tuning of the complex properties can allow the fluorophore to rebind the complex, displacing NO. The sensors have been found to detect NO in the μM range, but sensors with nM affinity would be useful for more widespread biological applications. Since water can compete with the fluorophore in binding to the transition metal, the sensors developed to date are not suitable for direct use in aqueous environments.¹⁴ However, the

¹⁰ (a) Nathan, C. *FASEB J.* **1992**, *6*, 3051-64. (b) Hibbs, J. B.; Taintor, R. R.; Vavrin, Z. *Science* **1987**, *235*, 4793-6.

¹¹ (a) Li, L.; Nicolson, G. L.; Fidler, I. J. *Cancer Res.* **1991**, *51*, 245-54. (b) Li, L.; Kilbourn, R. G.; Adams, J.; Fidler, I. J. *Cancer Res.* **1991**, *51*, 2531-5. (c) Dong, Z.; O'Brian, C. A.; Fidler, I. J. *J. Leuk. Biol.* **1993**, *53*, 53-60.

¹² (a) Barker, S. L.; Kopelman, R.; Meyer, T. E.; Cusanovich, M. A. *Anal. Chem.* **1998**, *70*, 971-6. (b) Barker, S. L.; Clark, H. A.; Swallen, S. F.; Kopelman, R.; Tsang, A. W.; Swanson, J. A. *Anal. Chem.* **1999**, *71*, 1767-72. (c) Barker, S. L.; Zhao, Y.; Marletta, M. A.; Kopelman, R. *Anal. Chem.* **1999**, *71*, 2071-5.

¹³ a) Hilderbrand, S. A.; Lim, M. H.; Lippard, S. J. *J. Am. Chem. Soc.* **2003**, *126*, 4872-4978. b) Franz, K. J.; Singh, N.; Spingler, B.; Lippard, S. J. *Inorg. Chem.* **2000**, *39*, 4081-4092. c) Franz, K. J.; Singh, N.; Lippard, S. J. *Angew. Chem., Int. Ed.* **2000**, *39*, 2120-2122.

¹⁴ Hilderbrand, S. A.; Lippard, S. J. *Inorg. Chem.* **2004**, *43*, 5294-5301

sensors can be surrounded by a NO-permeable/water-impermeable membrane (Silastic® Q7-4565 biomedical polymer) to sense NO without loss of stability (Figure 2).

A novel strategy for detecting NO has evolved in our laboratory using Cu^{2+} complexes.¹⁵ In the presence of excess NO, Cu^{2+} complexes are rapidly reduced to Cu^+ complexes (Figure 3). Applying this notion, we have developed fluorescent molecules with copper-binding groups and studied their reactions with nitric oxide. In the presence of Cu^{2+} , the complexes are quenched. The Cu^{2+} -bound complexes are reacted with NO, and the fluorescence is measured.¹⁶

Recent efforts in our laboratory have involved the investigation of π -conjugated polymers (CPs) (Figures 4-5) in NO sensing. These π -conjugated polymers can be highly fluorescent and organic- or water-soluble, with excitation wavelengths ranging from the UV to near-IR range. Swager, *et al.*, have found that the emission maxima of CPs can be tuned by changing side chain substitution, or altering the π -conjugated segments of the CP backbone. Since CPs are effective fluorescent sensors,¹⁷ they may be developed for the biological imaging of NO.

A nonionic, water-soluble CP has been developed by Swager, *et al.*¹⁸ This poly(phenylene ethynylene) (PPE) derivative contains hydrophilic hydroxyl and amide groups to facilitate dissolution of its hydrophobic backbone in aqueous media. Using this strategy, the water solubility of our previously developed polymer-based NO-sensing systems can be improved.¹⁹ Syntheses of the above water-soluble monomers have been undertaken. Future studies will involve the incorporation of Cu^{2+} -binding groups that will react with NO to afford Cu^{1+} complexes, with corresponding changes in fluorescence intensity.

¹⁵ Tran, D. and Ford, P. C. *Inorg. Chem.* **1996**, *35*, 2411-2412.

¹⁶ Smith, R. C. Unpublished results **2004**.

¹⁷ McQuade, D. T.; Pullen, A. E.; Swager, T. M. *Chem. Rev.* **2000**, *100*, 2537-2574.

¹⁸ Kuroda, K. Swager, T. M. *Chem. Commun.* **2003**, 26-27

¹⁹ Smith, R. C. Unpublished results **2004**.

Results and Discussion

Water-soluble PPE-based polymers (Figures 6-8) have been synthesized by Swager, *et al*, by the Sonogashira cross-coupling of monomers A (**6**) and B (**9**). Adapting previous routes, syntheses of **6** and **9** have been undertaken. As seen in Figure 6, ICl is added to dialkoxybenzene to give diiodoalkoxybenzene (**1**) in 85% yield. Compound **1** is then allowed to react with boron tribromide to afford 10.607 g (88%) of 2,5-diiodo hydroquinone (**2**). Ethyl bromoacetate is added to **2** to result in 5.195 g (40%) of (4-ethoxycarbonylmethoxy-2,5-diiodo-phenoxy)-acetic acid ethyl ester (**3**). Compound **4** is prepared in 49% yield by reacting **3** with diethanolamine, followed by triisopropylsilyl chloride (TIPSCl). Compound **5** is subsequently obtained by Sonogashira coupling of **4** and TMSA in 95% yield. Further applications of compound **5** are currently under investigation.

Hydrolysis of **3** affords 4.170 g (91%) of **7** as a light tan solid. Compound **7** is stirred with oxalyl chloride to create an acid chloride intermediate, which is added to diethyl iminodiacetate, and **8** is isolated in 72% yield. Monomer B (**9**) is synthesized by the condensation of Tris base with **8**, in an adaptation of Newkome's synthesis of arborols.²⁰ Monomer B is very soluble in water, DMSO, and DMF. After Monomer A (**6**) is synthesized, it will be polymerized by a Pd-catalyzed cross-coupling reaction with Monomer B and (*E, E*)-5,5'-bis(4-bromostyryl)-2-2'-bipyridine to obtain our target, a water-soluble polymer (**10**) (Figure 8). The optical properties of this water-soluble polymer, as well as its reactivity with various metal ions and nitric oxide are currently being studied.

The organic-soluble polymers **13** (Figure 9) and **16** (Figure 10) have also been synthesized through Suzuki and Sonogashira cross-coupling reactions, respectively. The quantum yield of **13** has been determined to be 0.17 in 4:1 CH₂Cl₂/MeOH, using quinine sulfate

²⁰ Newkome, G. R., Lin, X., Yaxiong, C., Escamilla, G. H. *J. Org. Chem.*, **1993**, *58*, 3123.

(QS) as a standard. This compound undergoes a 4-fold quenching after the addition of one equivalent of $\text{Cu}(\text{OTf})_2$ (Figure 11). Compound **16** has a higher high quantum yield ($\Phi_{\text{eff.}} = 0.27$) than **13** and undergoes 28-fold quenching after the addition of one equivalent of $\text{Cu}(\text{OTf})_2$ (Figure 12). No further quenching of CP1 or CP2 occurs after the addition of one equivalent of Cu^{2+} . Studies of the reactivity of Cu^{2+} -bound **13** and **16** to nitric oxide are currently in progress.

Conclusions

Two organic-soluble polymers, **13** and **16**, have been synthesized. Compound **16** has a higher quantum yield than **13** and the reactivity of its Cu^{2+} -bound complex to nitric oxide is currently under investigation. The synthesis of **10**, an aqueous-soluble polymer, is in progress, and will be followed by the characterization of its fluorescence properties and studies regarding its reactivity to nitric oxide.

Acknowledgements

I would like to thank Rhett Smith for providing compounds **4** and **5a**.

Experimental

Materials and Methods.

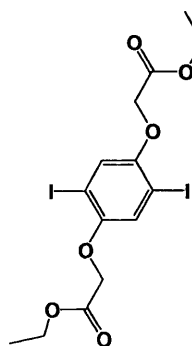
Reagents were purchased from Aldrich and used without further purification. THF and dichloromethane were obtained from a dry-still solvent dispensing system. Anhydrous DMF was purchased from Aldrich. Syntheses of compounds **1-9** were adapted from previous work by Swager, *et al.*¹⁹ Fluorescence spectra were acquired on a Hitachi F-3010 or a Photon Technology International (Lawrenceville, NJ) Quanta Master 4L-format scanning fluorimeter. Quantum yields were measured using a quinine sulfate standard ($\Phi_{QS} = 0.546$) and measurements were done in triplicate to ensure reproducibility. Fluorescence measurements assessing the reactivity of NO with polymers **13** and **16** were done using anhydrous, deoxygenated solvents and samples with an optical density of < 0.05 at the excitation wavelength. UV-visible absorption spectra were recorded on a Cary 1E UV-visible spectrophotometer at 25 °C. ¹H and ¹³C NMR spectra were acquired on a Varian 300 spectrometer.

Synthetic Procedures

Diiodoalkoxybenzene (1). Solid ICl (32.400 g, 0.200 mol) was added in portions to MeOH at 0 °C and stirred for five minutes until the reaction turned brown. Dialkoxybenzene (5.515 g, 0.040 mol) was added, and the brown slurry was heated to reflux for 4.5 h. The reaction was slowly cooled to 0 °C. Filtration and successive rinses with MeOH afforded 13.210 g (85%) of a white solid. MP: obs: 169.5-170.5 °C, literature: 171-172 °C. ¹H NMR (300 MHz, CDCl₃): δ 7.116 (s, 2H), 3.833 (s, 6H).

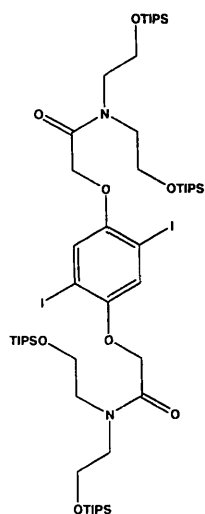
2,5-Diiodo Hydroquinone (2). Compound 1 (13.158 g, 0.033 mol) was cooled in 100 mL CH_2Cl_2 under N_2 , and a 1M solution of BBr_3 in CH_2Cl_2 (67.5 mL, 0.068 mol) was added slowly while stirring. The reaction was slowly warmed to room temperature and stirred for 48 h. The reaction was then quenched with 40 mL H_2O . Aqueous portions were washed with ether, and organic portions were washed with 2N NaOH , evaporated, and dried under vacuum to afford 10.607 g (88%) of product. $^1\text{H NMR}$ (300 MHz, CDCl_3): δ 7.23, (s, 2H), 4.90 (s, 2H).

(4-Ethoxycarbonylmethoxy-2,5-diiodo-phenoxy)-acetic acid ethyl ester (3).



Ethyl bromoacetate was added dropwise to a suspension of 2 (10.607 g, 0.029 mol) and K_2CO_3 (20.401 g, 0.150 mol) in acetone. The reaction was heated to reflux overnight, evaporated, and recrystallized from EtOH to yield 5.195 g (40%) of product. $^1\text{H NMR}$ (300 MHz, CDCl_3): δ 7.167, (s, 2H), 4.623 (s, 2H), 4.302 (q, 4H), 1.321 (t, 6H).

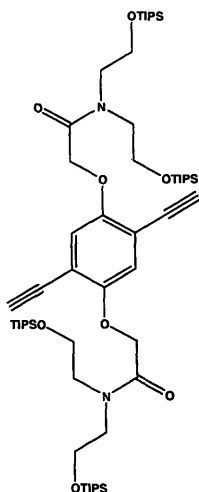
2-(4-{{Bis-(2-triisopropylsilyloxy-ethyl)-carbamoyl}-methoxy}-2,5-diiodo-phenoxy)-N,N-bis-(2-triisopropylsilyloxy-ethyl)-acetamide (4).



Compound 3 (2.000 g, 3.74 mmol) was heated to reflux with diethanolamine (1.580 g, 15 mmol) in 25 mL of ethanol overnight. The reaction was evaporated and dried under vacuum. The solid was suspended in 190 mL of THF, and imidazole (2.549 g, 37.5 mmol) and TIPSCl (7.200 g, 37.5 mmol) were added. The reaction was stirred overnight at RT. The solvent was removed by rotary evaporation. The residue was purified through silica gel column chromatography and recrystallization from $\text{CH}_2\text{Cl}_2/\text{MeOH}$ to afford 2.350 g (49%) of a white

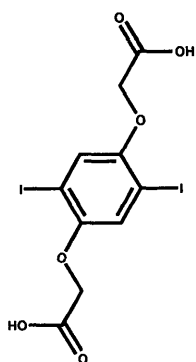
crystalline solid. $^1\text{H NMR}$ (300 MHz, CDCl_3): δ 7.266, (s, 2H), 4.814 (s, 4H), 3.882 (q, 8H), 3.683 (t, 4 H), 3.585 (t, 4H), 1.050 (m, 84H).

Compound 5.



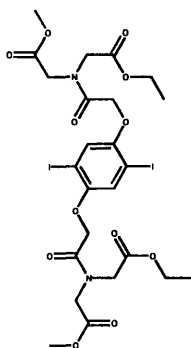
Compound 4 (0.980 g, 0.76 mmol) and CuI (3 mg, 0.02 mmol) were dissolved in 2 mL isopropylamine and 6 mL toluene in a Schlenk flask. The reaction mixture was degassed by three quick vacuum and back-filled with Ar cycles. $\text{Pd}(\text{PPh}_3)_4$ (36 mg, 0.03 mmol) and TMSA (200 mg, 1.17 mmol) were added to the flask under Ar. After heating at 50°C overnight, the solvent was evaporated. The residue was dissolved in CH_2Cl_2 , washed with NH_4Cl (aq) solution, and dried over MgSO_4 . The crude residue was recrystallized with 1:1 $\text{CH}_2\text{Cl}_2/\text{MeOH}$ to afford 0.775 g (95%) of product. $^1\text{H NMR}$ (300 MHz, CD_2Cl_2): δ 6.88 (s, 2H), 4.82 (s, 4H), 3.85 (t, 8H), 3.63 (t, 4H), 3.55 (t, 4H), 1.05 (m, 84H), 0.24 (s, 18H).

2-(4-{{Bis-(2-triisopropylsilyloxy-ethyl)-carbamoyl}-methoxy}-2,5-diethynyl-phenoxy)-N,N-bis-(2-triisopropylsilyloxy-ethyl)-acetamide (7).



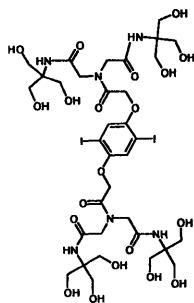
Compound 3 (5.557 g, 0.010 g) was heated to reflux in 194 mL MeOH with NaOH (11.640 g, 0.291 mol) for 2.5 h. The reaction was cooled to RT and the solvent was evaporated. The resulting residue was acidified with 1 N HCl (aq), and a white precipitate formed, which was collected by centrifugation, and washed with H_2O until the solution was pH 4. The residue was lyophilized overnight to afford a light tan solid (4.170 g, 91%). $^1\text{H NMR}$ (300 MHz, $\text{DMSO}-d_6$): δ 7.2 (s, 2H), 4.7 (s, 4H).

2-(4-{{Bis-(2-hydroxy-ethyl)-carbamoyl}-methoxy}-2,5-diethynyl-phenoxy)-N,N-bis-(2-hydroxy-ethyl)-acetamide (8).



Compound 7 (3.000 g, 6.3 mmol) was stirred in 20 mL oxalyl chloride and heated to reflux overnight. Excess oxalyl chloride was evaporated and the residue was dissolved in 20 mL CH₂Cl₂. The reaction was cooled to 0 °C, and a diethyl iminodiacetate solution (4.800 g, 25 mmol in 20 mL CH₂Cl₂ and 2.7 mL Et₃N) was added dropwise. The solution was warmed to room temperature and stirred overnight. The reaction was then washed with 1N NaOH, 1N HCl, sat. NaCl (aq), and dried over MgSO₄. The solvent was evaporated to afford 3.613 g (72%) of desired product. ¹H NMR (300 MHz, CDCl₃): δ 7.2 (s, 2H), 4.7 (s, 4H), 4.3 (s, 4H), 4.2 (m, 12H), 1.3 (t, 12H).

Monomer B: (4-Carboxymethoxy-2,5-diiodo-phenoxy)-acetic acid (9).



Compound 8 (1.000 g, 1.24 mmol), Tris (0.602 g, 4.97 mmol), and K₂CO₃ (0.687 g, 4.97 mmol) were suspended in 10 mL DMSO and stirred overnight. Excess potassium carbonate was filtered and the filtrate was vacuum distilled. The oily brown residue was rinsed with CH₂Cl₂, and a hefty amount of tan-colored precipitate formed. The precipitate was collected by centrifugation and dried under vacuum. The residue precipitates out of dichloromethane as a light pink solid, and appears to be very hydroscopic. ¹H NMR (300 MHz, DMSO-*d*₆): δ 7.723 (bs, 2H), 7.424 (bs, 2H), 7.246 (bs, 2H), 4.852 (bs, 4H), 4.596 (bs, 12H), 4.073 (bs, 4H), 3.955 (bs, 4H), 3.565 (bs, 24H).

Polymer Synthesis

Synthesis of Tetrakis(triphenylphosphine) Palladium(0) Catalyst. PdCl₂ (1 g) was placed in a 3-neck round-bottom flask with a thermometer and a filter stick attached to a second inverted 3-necked round-bottom flask. DMSO (68 mL) and triphenylphosphine (7.400 g) were added, and the reaction was heated to 140 °C with stirring. The reaction was removed from heat, and stirred for 15 more minutes. Hydrazine hydrate (1.4 mL) was added rapidly, and the reaction was allowed to cool to room temperature. The apparatus was inverted for filtration, and the solid was washed with ethanol (2 x 10 mL) and dry ether (2 x 10 mL), producing a yellow solid, which was dried under vacuum for 3.5 h.

Polymer 1: Suzuki Coupling of (11) and (12). Compound 11 (0.041 g, 0.1 mmol), 12 (0.074 g, 0.15 mmol), 6, 6'-dibromo-2, 2'-6, 2''-terpyridine (0.0196 g, 0.05 mmol), cesium carbonate (0.013 g, 0.45 mmol) and Pd(PPh₃)₄ (0.048 g, 0.045 mmol) were combined in DMF under N₂. The reaction was stirred at 100 °C for 48 h. Organic layers were washed with saturated EDTA (aq), and aqueous layers were washed with CH₂Cl₂. The organic layers were combined, evaporated, and washed with water and MeOH.

Polymer 2: Sonogashira Coupling of (14) and (15). Compounds 14 (0.044 g, 0.1 mmol), 15 (0.033 g, 0.15 mmol), 6, 6'-dibromo-2, 2'-6, 2''-terpyridine (0.0196 g, 0.05 mmol), CuI₂ (0.014 g, 0.045 mmol), and 10% Pd(PPh₃)₄ (0.048 g, 0.045 mmol) were stirred in 2.5 mL of diisopropylamine and 8 mL of toluene. The reaction was heated in a sealed pressure tube at 80°C for 24h. Organic layers were washed with saturated EDTA (aq), and aqueous layers were washed with CH₂Cl₂. The organic layers were combined, evaporated, and washed with water and MeOH.

Fluorescence Experiments of Polymers 1 and 2

Titration of (13) with Cu(OTf)₂ (Figure 11). A 5.0 μM solution of (13) was prepared in 4:1 CH_2Cl_2 :EtOH. A 3 mL aliquot of the solution was added to a quartz cell with an optical pathlength of 1 cm. Small (5 - 160 μL) aliquots of a 1.6×10^{-4} M Cu(OTf)₂ solution were added to the sample cell, and the fluorescence was monitored at an excitation wavelength of 344 nm. The integrated fluorescence intensity was observed to have a 4-fold decrease in integrated fluorescence, upon addition of 1 equivalent of Cu^{2+} . No further quenching was observed after a second equivalent of Cu^{2+} was added.

Titration of (16) with Cu(OTf)₂ (Figure 12). A 0.48 μM solution of (16) was prepared in 4:1 CH_2Cl_2 :EtOH. A 3 mL aliquot of the solution was added to a quartz cell with an optical pathlength of 1 cm. Small (10 – 110 μL) aliquots of a 1.6×10^{-5} M Cu(OTf)₂ solution were added to the sample cell, and the fluorescence was monitored at an excitation wavelength of 393 nm. The integrated fluorescence intensity was observed to have a 28-fold decrease in integrated fluorescence, upon addition of 1 equivalent of Cu^{2+} . No further quenching was observed after a second equivalent of Cu^{2+} was added.

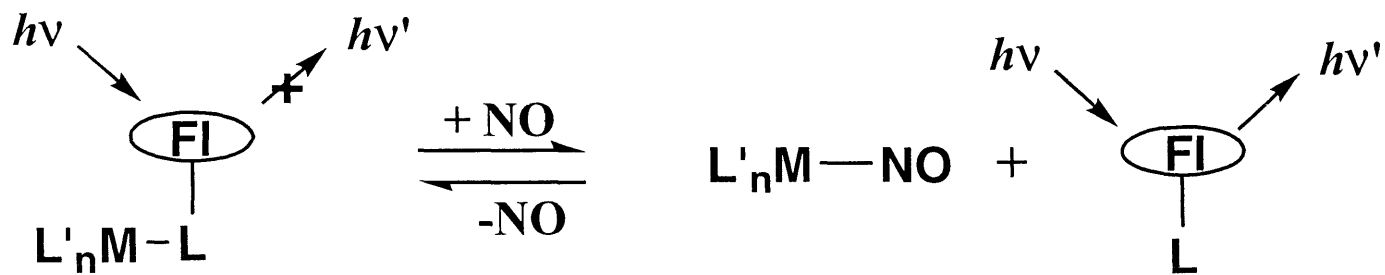


Figure 1: NO Detection by Fluorophore Displacement

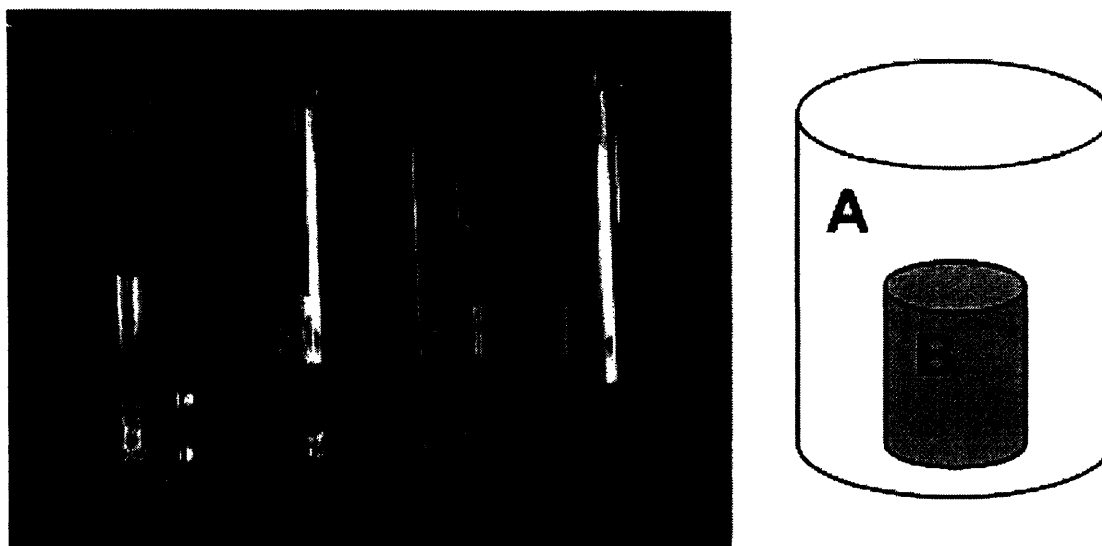


Figure 2: Silastic® Membranes Applied In Aqueous NO Sensing.¹⁴
 The left vial contains a 15 mL saturated NO solution in an aqueous environment. Silastic® membrane separates vials A and B. The right vial contains 1.5 mL of a CH₂Cl₂ solution of 40 μM [Rh2[μ-O₂CMe)₄] and 20 μM Ds-pip.

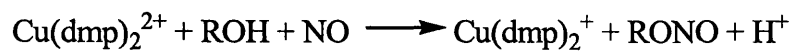
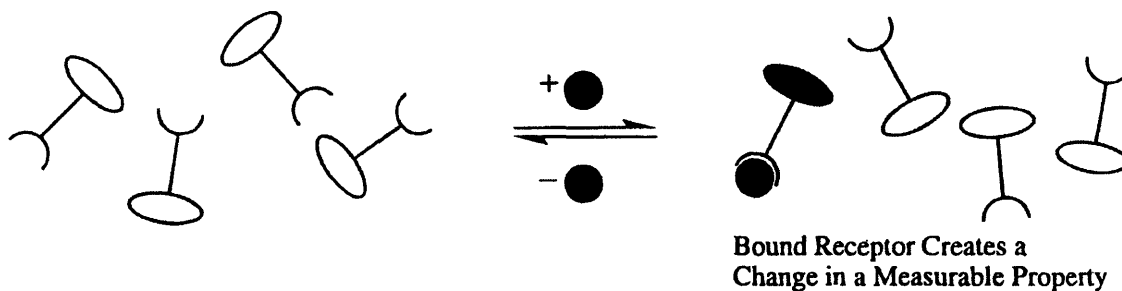


Figure 3: Reduction of Cu²⁺ to Cu¹⁺ by Nitric Oxide in an Alcoholic Solvent¹⁵

Traditional Chemosensor:

Sensitivity related to the equilibrium constant $K(\text{eq}) = \frac{[\text{Bound Receptor}]}{[\text{Unbound Receptor}][\text{Analyte}]}$



Receptors Wired in Series:

Amplification due to a collective system response.

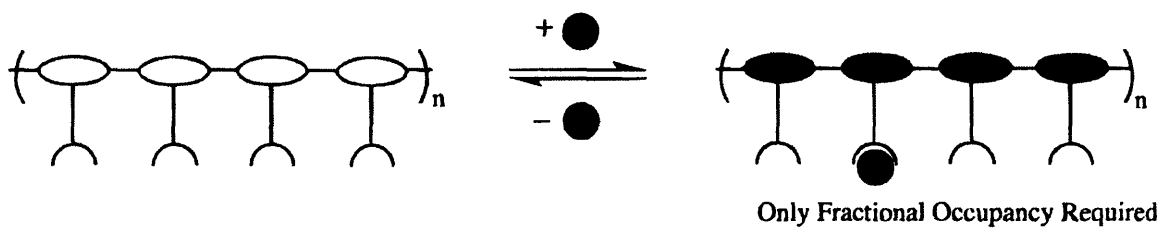


Figure 4: Small Molecule Chemosensors (above) and Conjugated Polymer Sensors (below)²¹

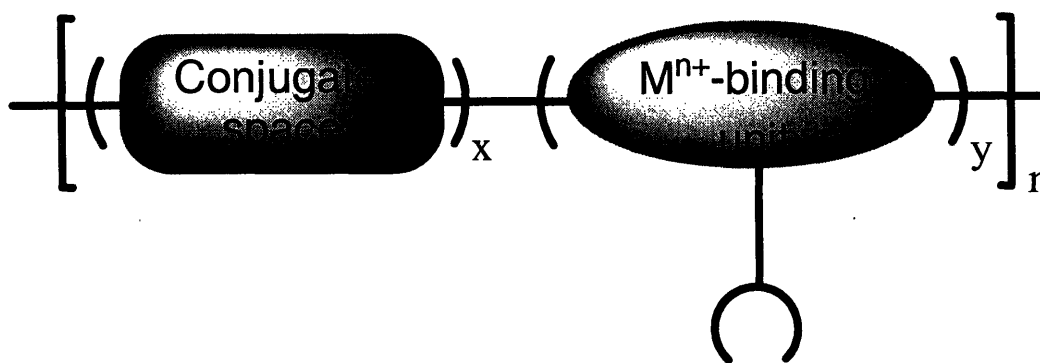


Figure 5: Conjugated Polymers as NO Sensors

²¹ Swager, T. M. *Acc. Chem. Res.* **1998**, *31*, 201-207.

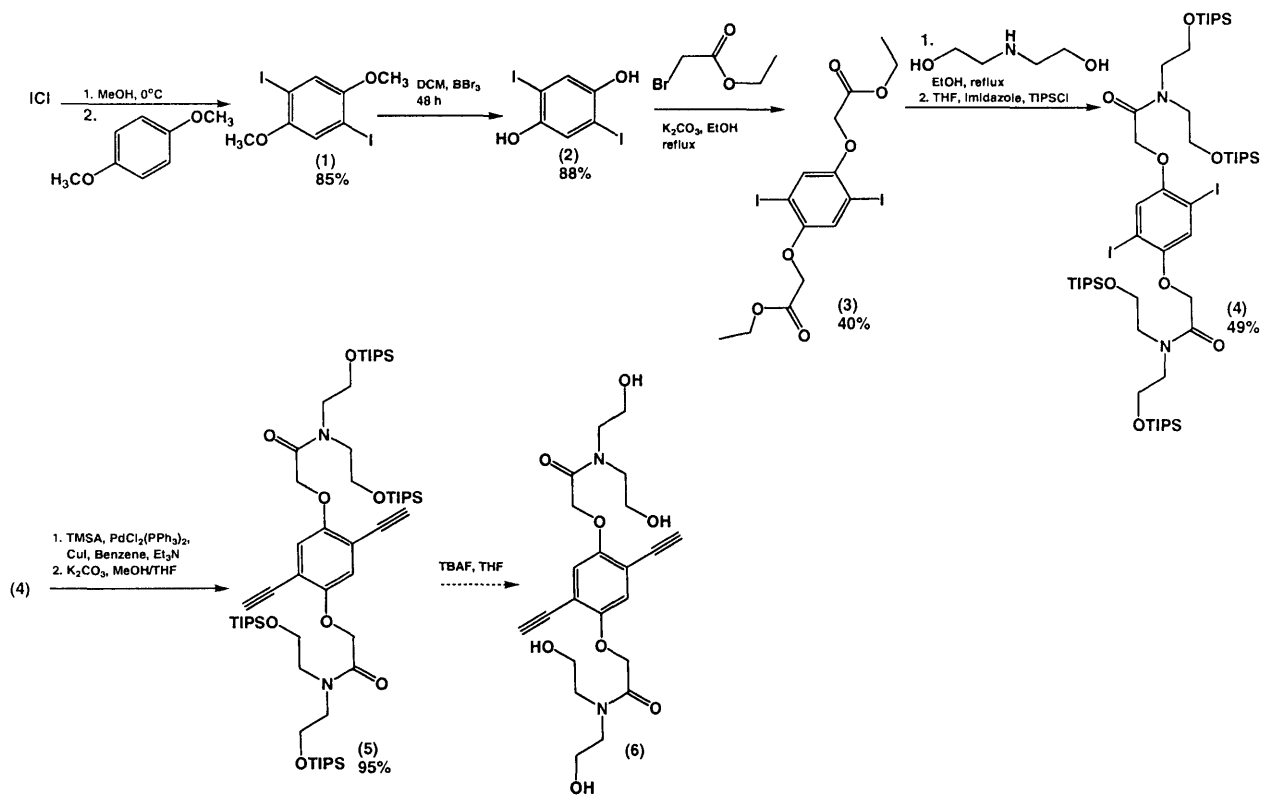


Figure 6: Synthetic Route Used to Prepare Monomer A

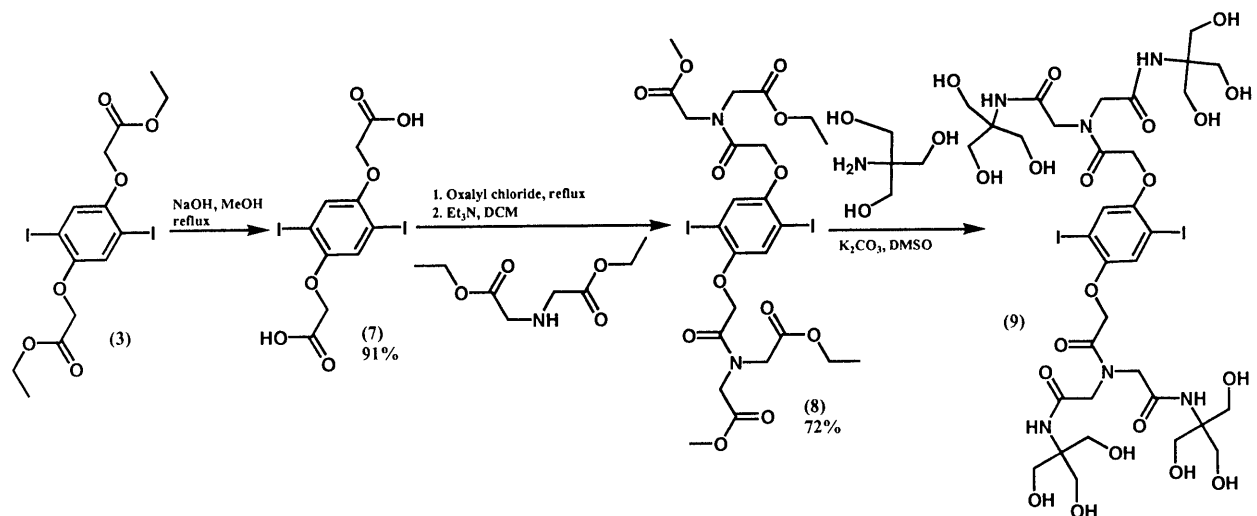


Figure 7: Synthetic Route Used to Prepare Monomer B

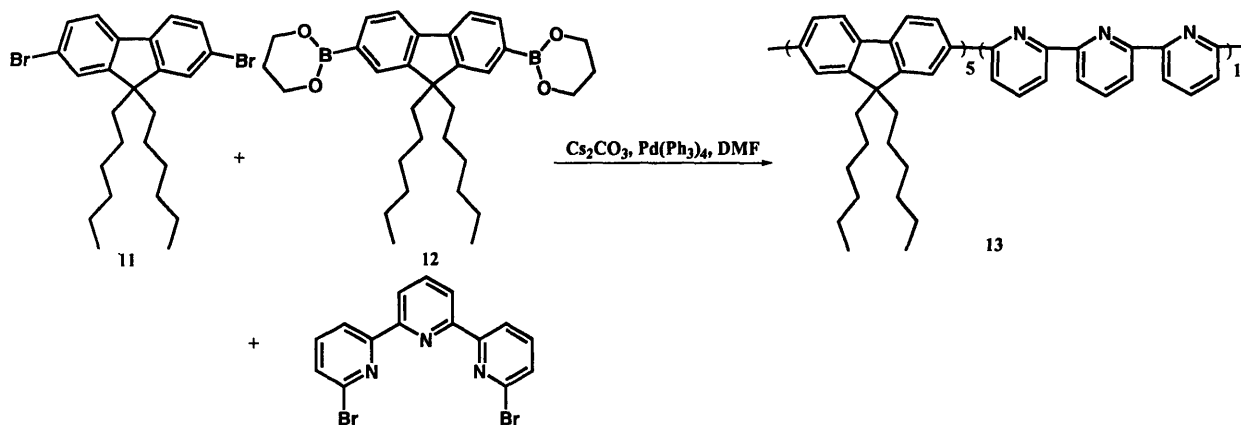


Figure 9: Synthesis of 13 Through A Suzuki Coupling Reaction

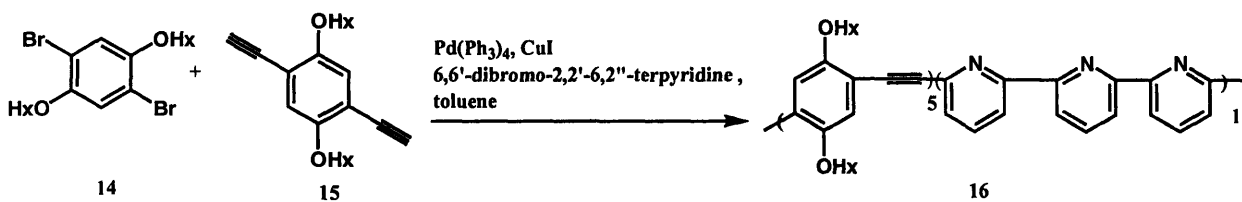


Figure 10: Synthesis of 16 Through a Sonogashira Coupling Reaction

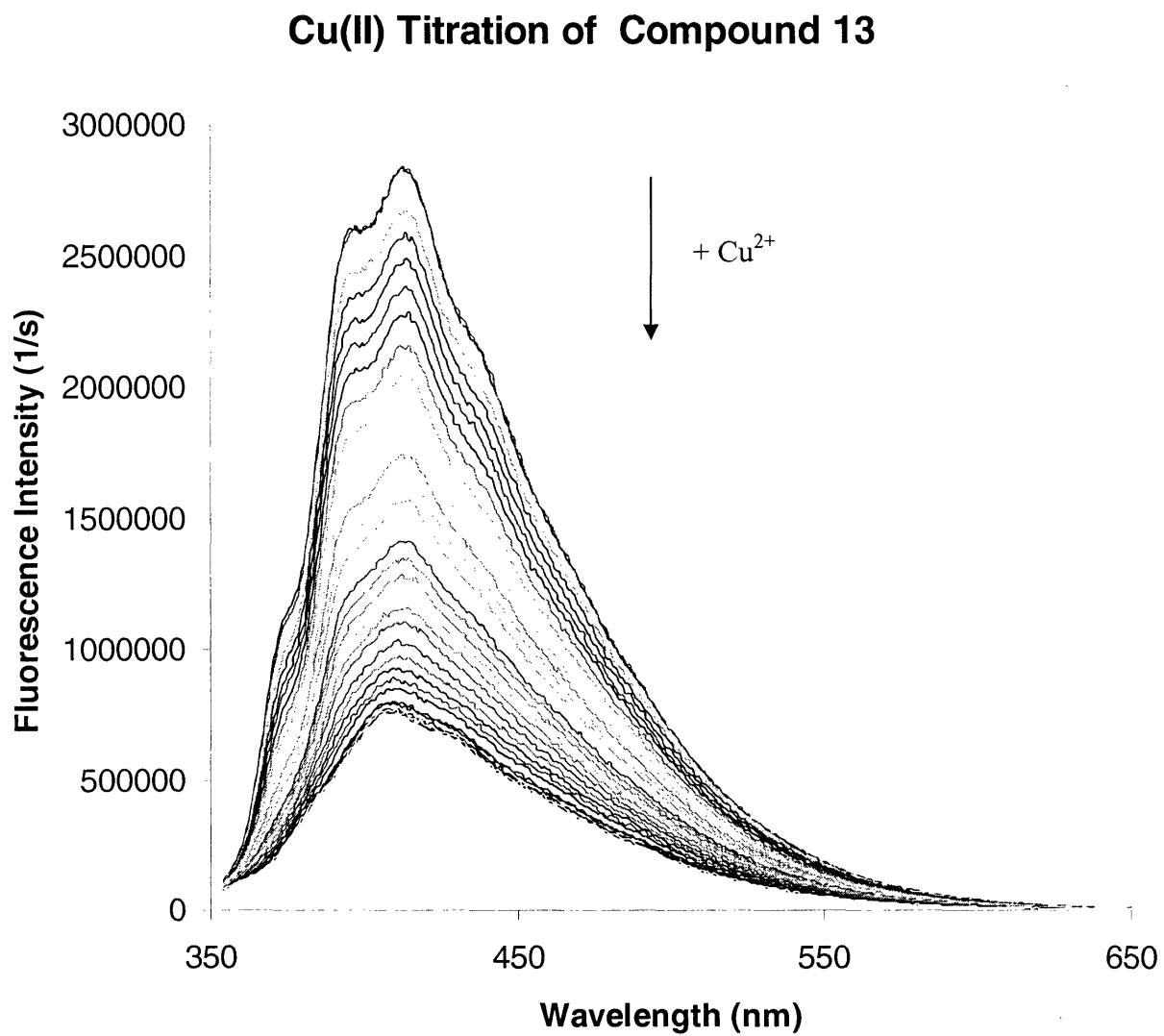


Figure 11: Cu(II) Titration of Compound 13

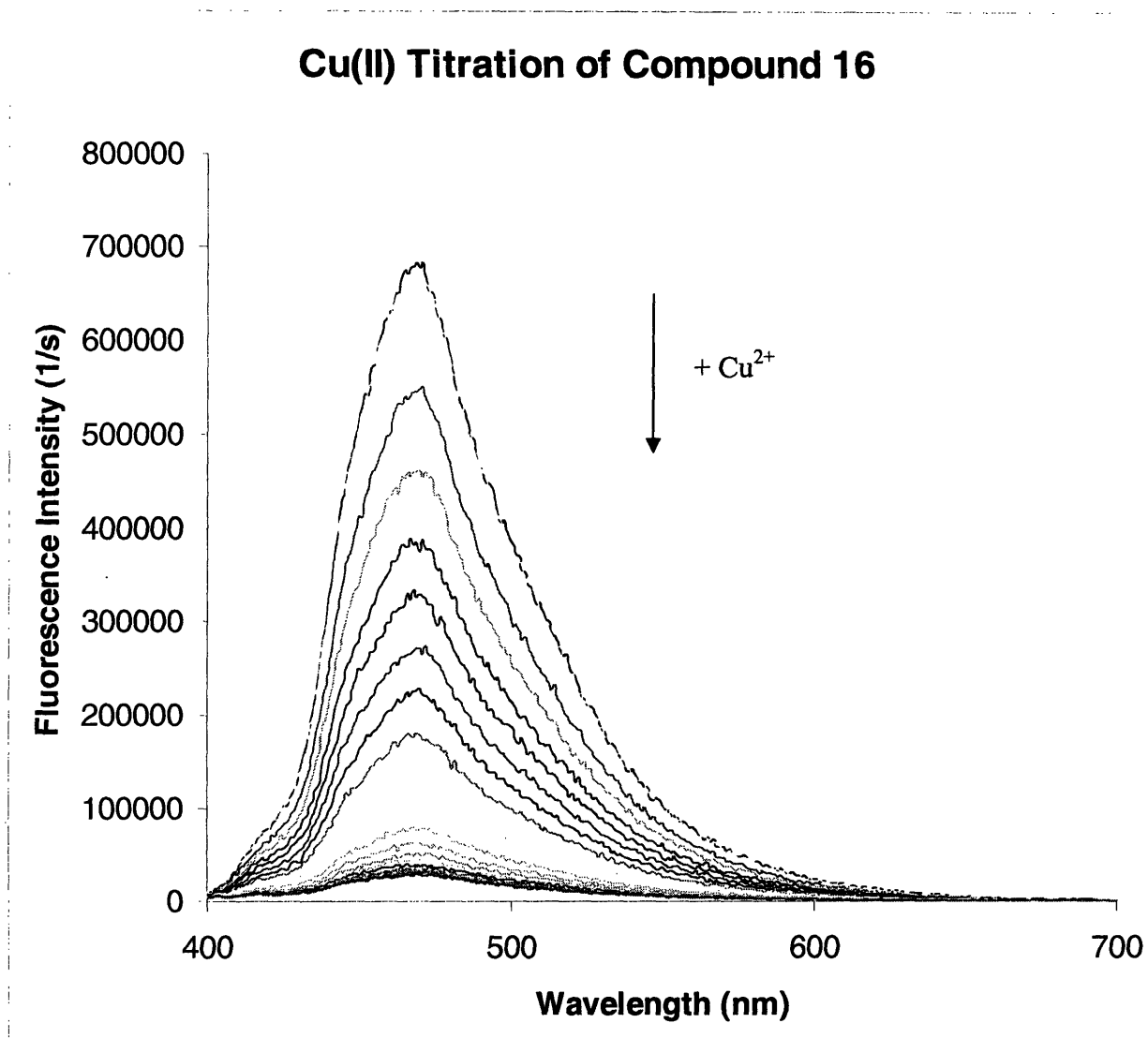


Figure 12: Cu(II) Titration of Compound 16

Biographical Note

Annie Won was born on March 9, 1983 in Long Branch, NJ and attended Monmouth Regional High School before entering MIT in 2001. She was initially a brain and cognitive sciences major (course 9) who had done UROPs in the Corkin and Adelson labs, and changed majors to chemistry (course 5) in the second semester of her junior year, with the possibly insane intention of graduating by 2005. During her stay here, Annie has lived in four dorms (Next House, Tang Hall, French House (LMF), and the Warehouse). Annie has done several activities during her stay here, including the following: IM tennis and IM ice hockey (affording her a sexy neck brace for a brief period of time), and Rune (editor-in-chief for a couple years). She is also an arts scholar, has served as both LMF social and athletics chairs, and has spent a little time serving on various GRT selection committees. In the free time she cannot afford, she writes, draws caricatures, and claims to still play the piano. Annie will be pursuing graduate studies in organic chemistry at the University of Illinois Urbana-Champaign in the coming fall.

Curriculum Vitae

- EDUCATION:** **Massachusetts Institute of Technology** **Cambridge, MA**
2001-2005. Candidate for Bachelor of Science Degree in Chemistry,
June 2005.
- Monmouth Regional High School.** **Tinton Falls, NJ**
1997-2001. Class of 2001 Valedictorian
- New Jersey Governor's School of the Sciences** **Madison, NJ**
2002. One-month intensive research program at Drew University.
- RESEARCH:** **Massachusetts Institute of Technology** **Cambridge, MA**
Lippard Laboratory, Neurochemistry Group.
Undergraduate Researcher.
Summer 2003-Spring 2005. Syntheses of zinc and nitric oxide sensors.
- Massachusetts Institute of Technology** **Cambridge, MA**
Perceptual Science Group
Undergraduate Researcher
Fall 2002-Spring 2003. Psychophysics studies involving the creation of a
database of illumination maps.
- Massachusetts Institute of Technology** **Cambridge, MA**
Behavioral Neuroscience Laboratory
Undergraduate Researcher.
Spring-Summer 2002. Studies regarding the neurological basis of memory.
Transcribed interviews, and designed pilot tests regarding long- and short-
term semantic memory.
- AWARDS:** Arts Scholar, National Council of Teachers of English Achievement Award in
Writing, National Honor Society Scholarship, Goldman Sachs – Walter F.
Blaine Scholarship
- ACTIVITIES:** Rune (MIT Journal of Arts and Letters): staff member (2001-2002), editor-in-
chief (2002-2004); MIT Arts Scholar (2003-present]; Lippard Group IM Ice
Hockey (2003-2004); French House GRT Selection committee (2003-2004);
MIT Chinese Students Club (2001-2003); French House Social Chair (2002-
2003); French House Athletics Chair (2002-2003); Next House GRT
Selection Committee (2002); Next House Intramural Tennis: doubles (2001-
2002).
- PUBLICATIONS:** Woodrooffe, Carolyn C.; Won, Annie C.; Lippard, Stephen J. Esterase-
Activated Two-Fluorophore System for Ratiometric Sensing of Biological
Zinc(II). *Inorg. Chem.* **2005**, *44*, 3112-3120.